DELAYED DYNAMICS OF SEAIR MODEL FOR COVID-19 WITH VACCINATION

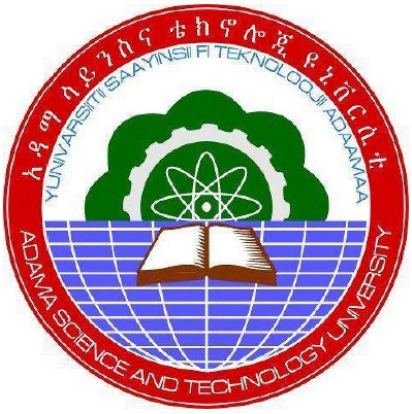

Boka Mezgebu Tasisa

A Thesis Submitted to Department of Applied Mathematics

School of Applied Natural Science,

Presented in Partial Fulfillment of the Requirement for the Degree of Master's in Applied Mathematics

Office of Graduate Studies

Adama Science and Technology University

October 10, 2022

Adama, Ethiopia

DELAYED DYNAMICS OF SEAIR MODEL FOR COVID-19 WITH VACCINATION

Boka Mezgebu Tasisa

Advisor: Legesse Lemecha(Ph.D.)

Co-Advisor: N. Seshagiri Rao(Ph.D.)

A Thesis Submitted to Department of Applied Mathematics

School of Applied Natural Science

Presented in Partial Fulfillment of the Requirement for the Degree of Master's in Applied Mathematics

Office of Graduate Studies

Adama Science and Technology University

October 10, 2022

Adama, Ethiopia

Declaration

I hereby declare that this Master Thesis entitled **“Delayed Dynamics of SEAIR Model for COVID-19 with Vaccination"** is my original work. That is, it has not been submitted for the award of any academic degree, diploma or certificate in any other university. All sources of materials used for this thesis have been duly acknowledged through appropriate citations.

Name of Student	Signature	Date

Recommendation of Advisors

We, the advisors of this thesis, hereby certify that we have read the revised version of the thesis entitled ***"Delayed Dynamics of SEAIR Model for COVID-19 with Vaccination"*** prepared under our guidance by ***Boka Mezgebu Tasisa*** submitted in partial fulfillment of the requirements for the degree of Master's of Science in Applied Mathematics. Therefore, we recommend that the submission of revised version of the thesis to the department following the applicable procedures.

Major Advisor	Signature	Date
Co-advisor	Signature	Date

Approval Page

We, the advisors of the thesis entitled ***"Delayed Dynamics of SEAIR Model for COVID-19 with Vaccination"*** and developed by ***Boka Mezgebu***, hereby certify that the recommendation and suggestions made by the board of examiners are appropriately incorporated into the final version of the thesis.

Major Advisor	Signature	Date
Co-Advisor	Signature	Date

We, the undersigned, members of the Board of Examiners of the thesis by Boka Mezgebu have read and evaluated the thesis entitled ***"Delayed Dynamics of SEAIR Model for COVID-19 with Vaccination"*** and examined the candidate during open defense. This is, therefore, to certify that the thesis is accepted for partial fulfillment of the requirement of the degree of Master of Science in Applied Mathematics.

Chair person	Signature	Date
Internal Examiner	Signature	Date
External Examiner	Signature	Date

Final approval and acceptance of the thesis is contingent upon submission of its final copy to the Office of Postgraduate Studies (OPGS) through the Department Graduate Council (DGC) and School Graduate Committee (SGC).

Department Head	Signature	Date
School Dean	Signature	Date
Office of Postgraduate Studies, Dean	Signature	Date

Acknowledgement

First and foremost, I express my heartfelt gratitude to Almighty God for being the source of all innovations and for providing me with the health and wisdom to carry on with my daily activities.

Next, I'd like to express my sincere gratitude to my advisor, Dr. Legesse Lemecha, for his kind encouragement, direction, support, and oversight of my academic career at Adama Science and Technology University. Your advice throughout the program was excellent, and I hope you'll keep sharing your wealth of knowledge and experience with me after it's over. God will repay you, and I will never stop praying that he receives a mighty blessing as he continues to assist other students.

In addition, I want to thank my co-advisor, Dr. N. Seshagiri Rao, for his encouragement and assistance throughout my academic career. My sincere gratitude is extended to my former advisor, Dr. Shifera Feyisa, for his direction, assistance, and encouragement throughout the title selection process up until his soul's departure. God bless him and his family. Peace be upon their souls. I'll keep following his instructions. I also want to thank the lab staff and all the instructors for helping me complete this work.

My sincere gratitude goes out to my entire family for their understanding, patience, and support throughout the program. Last but not least, I want to thank everyone who has helped me in any way during my struggle to reach this academic level.

Table of Contents

List of Tables

List of Figures

Acronyms

COVID-19	Corona Virus Infectious Diseases-2019
CFEP	COVID Free Equilibrium Point
DDEs	Delay Differential Equations
EEP	Endemic Equilibrium Point
MERS	Middle East Respiratory Syndrome
ODEs	Ordinary Differential Equations
SARS	Severe Acute Respiratory Syndrome
SARS-COV-2	Severe Acute Respiratory Syndrome Coronavirus-2
WHO	World Health Organization

Abstract

COVID-19 is an infectious disease caused by SARS-CoV-2, a virus that belongs to the coronavirus subfamily, a collection of connected RNA viruses. It has affected many countries globally, including Ethiopia. This study aims to develop and analyze a mathematical model of COVID-19 transmission dynamics and apply it as a case study in Ethiopia. For this , a system of non-linear ordinary differential equations has been used to formulate a deterministic mathematical model with six compartments to describe the dynamics of the COVID-19 infection. We investigated the model's dynamical behavior and carried out a qualitative analysis. The system has two equilibrium points, the endemic equilibrium point and the disease free equilibrium point. Utilizing the next-generation matrix, the fundamental reproduction number R_0 *was calculated, and the stability of the equilibrium points was examined. According to the qualitative analysis, the disease-free equilibrium point is stable both locally and globally if* $R_0 < 1$*, and the endemic equilibrium point is similarly stable both locally and globally if* $R_0 > 1$ *in certain circumstances. Additionally, bifurcation analyses have been carried out to reveal the dynamics of coronavirus disease transmission. The COVID-19 prediction is more accurate when the time delay period is included in the model. A logical and more accurate representation of the SVEAIR model was created by adding a delay period for incubation. The dynamical behavior of the model will not match the current situation without the delay period. A stability loss of the endemic equilibrium point at* $R_0 > 1$ *and approaches to the disease free equilibrium point resulted from the effect of incubation time. The Hopf bifurcation phenomenon can alter the system's behavior and cause periodic oscillations. The qualitative analysis of the newly developed SVEAIR model is proven by comparing its predictions with the data collected from the Ethiopian Minister of Health. Finally, numerical simulation is presented using Mathlab2017b software to check the validity of the analytical results presented in the two models.*

Keywords:Mathematical Modeling; SVEAIR model; COVID-19; stability analysis; sensitivity analysis; Delayed SVEAIR model.

CHAPTER 1

INTRODUCTION

1.1 Back ground of the study

SARS-CoV-2, as a novel coronavirus, was first identified by the Chinese authorities in Wuhan, Hubei Province of China, which has caused the pneumonia (COVID-19) outbreak in China and other countries (WHO, 2020b). COVID-19 remains an on-going global pandemic at present. It has created one of the biggest challenges in the history of mankind. With over 270 million positive cases and over 5 million deaths up to December 15, 2021, according to the WHO report, COVID-19 continues its deadly killing spree in all corners of the world.

Coronavirus diseases are brought on by viruses that belong to the coronavirus subfamily, a collection of connected RNA viruses that affect both mammals and birds. This category of viruses can cause mild to fatal respiratory tract infections in both people and birds. Some common cold instances in humans (which are also brought on by other viruses, primarily rhinoviruses) are milder than others, although more deadly cases can result in SARS, MERS, and COVID-19 (Palmenberg et al., 2009). 45 species are listed as coronaviruses as of 2021 (Alfarouk et al., 2021). Coronaviruses are recognized for their structural features that resemble stellar coronas, such as the corona of the Sun that may be seen during a total solar eclipse; corona is derived from the Latin term corona, which means "garland, wreath, or crown." The term was originally used in a Nature article in 1968 (Almeida et al., 1968), invented by Tony Waterson during a meeting with his colleagues June Almeida and David Tyrrell, the pioneers of coronavirus investigations, and approved by the International Committee for the Nomenclature of Viruses three years later.

Lalchhandama (2020), the first coronavirus disease, was discovered in the late 1920s;

however, the most recent common ancestor of coronaviruses is thought to have existed as recently as 8000 BCE. In the 1960s, several experiments in the United States and the United Kingdom led to the discovery of human coronaviruses (Wertheim et al., 2013). Bats are frequently cited as the source of human coronaviruses (Monto, 1989). An outbreak of a fatal disease known as COVID-19 that started at the end of December 2019 has upset numerous global institutions, including transportation (air, marine, and land), the economy, educational systems, sports, and entertainment, among many others (Forni et al., 2017). Many people have died and been infected, and they are fighting for their lives in various hospitals around the world (Forni et al., 2017).

The origin, behavior, patterns of dissemination, and many other biological details surrounding the COVID-19 outbreak are still largely unknown. In several branches of science, technology, and engineering, researchers have redirected their efforts toward comprehending and battling this new threat to civilization. Research to develop a novel and effective vaccination is ongoing in numerous laboratories across many different nations. In several nations, the use of ventilators and numerous other items to help some people recover has yielded some excellent results. Mostly through little droplets spread through coughing, sneezing, or talking, the disease can spread from person to person. Additionally, contaminated surfaces might spread the disease to susceptible people. Fever, weariness, a dry cough, exhaustion, and shortness of breath are the most typical COVID-19 signs and symptoms (Centers et al., 2020). A few patients may experience diarrhea, sore throats, running noses, congestion, or aches and pains. The signs are often not severe, although they may get worse with time. As preventive measures, it is advised to wash your hands frequently, cover your mouth or nose when you cough or sneeze, refrain from touching your eyes, nose, or mouth, and keep social distance to avoid infection.

Many nations have taken significant measures to stop the spread of the COVID-19 epidemic and, more importantly, to safeguard healthcare systems as a result of its severity. Public events were canceled; schools, public places, and borders were closed; there were travel prohibitions; there was a lockdown, etc., among other decisions. Those nations that adopted these techniques first have reaped the greatest rewards from them. While these tactics were beneficial, socio-economic harm was nevertheless done as a result of them. In reality, social isolation, anxiety about the future, and an increase in spousal violence have all been factors contributing to mental health problems during the lockdown. Many workers' jobs

have been lost. Supply networks were disturbed by business shutdowns, which reduced productivity.

Mathematical modeling is an essential theoretical framework to understand the mechanism of spread of disease. This is a useful tool for presenting COVID-19 broadcasts. Global attempts to model dynamics and important transmissions should be identified. Such theoretical methods may offer additional recommendations for estimating the model's parameters and forecasting this spread. Many mathematical models suggest that locking down is the most effective way to reduce the spread of COVID-19 among the aforementioned control methods. However, lockdown interventions are very risky for a country's economic stability. Therefore, instead of imposing lock down in their countries, social distanceing interventions to reduce the successful contact of illnesses and rapid-testing to map the spread of infection are being considered as solutions in various countries as a measure to prevent the rising number of infections. Basic imitation numbers and serial intervals are examined using mathematical modeling. Although there are numerous mathematical models for coronavirus disease prediction available online, these models still need to be improved in order to effectively manage the virus's spread.

Understanding the mechanisms of how a disease like COVID-19 spreads among humans requires the use of mathematical models. With the help of these models, health professionals and policy makers can better understand how infectious diseases spread and take steps to stop their wide-scale spread. Over the past century, substantial research has been done on mathematical models of the dynamics of infectious diseases (Kermack & McKendrick, 1927; Hethcote, 2000). They are based on the SIR model.

The production value "R_0", which gauges a virus capacity for transmission, is a dimensionless constant used to limit the spread of viruses. The R_0 value differs from virus to virus (the R_0 value for influenza transmission, for instance, is 3 (Anderson & May, 1992)). An infectious disease is likely to progress more slowly when $R_0 < 1$ affects just less than one individual. To connect epidemic patterns, more theoretical work is needed as R_0 alone only offers limited insight into the possibility for the transmission of infectious diseases (Davis et al., 2008; Salkeld et al., 2010). Further theoretical work is needed to connect the patterns of an epidemic.

Recent studies on COVID-19 (Maleewong, 2020; Menendez, 2020; Ivorra et al., 2020) have been helpful to gain insights into the transmission dynamics and potential role of different intervention strategies such as mitigation and suppression to slow down the epidemic spread, reduce the peak health care to protect those who are most at risk from infections, and reducing the number of infective cases to the low level, as well as enforcing lock down to region of highly infective cases, home isolation of suspect cases, home quarantine of those living in the same household, and implementing social distancing among individuals. COVID-19 is a newly emergent virus, and much remains to be understood about its transmission.

Since the outbreak of the disease, various mathematical models have been proposed and analyzed to explore the consequences of the transmission dynamics of COVID-19 among the population. However, as we discussed above, the vaccinated class does not considered. The COVID-19 vaccine is available today in every country. Ghostine et al. (2021) introduced a vaccinated class in the model even though asymptomatic infected and time delay was not considered in the model formulation. Çakan (2020) investigated mathematical models of the SEIR type with time delay. Hence, the model did not consider the asymptomatic infected and vaccinated classes. As a result, introducing the vaccinated class is a critical compartment for studying COVID-19. In the present thesis, we analyzed the transmission dynamics of COVID-19 using a mathematical model by classifying populations into susceptible,vaccinated, exposed, asymptomatic infected, symptomatic infected, and recovered with appropriate assumptions. Then we extended the model to delay model.

1.2 Statement of the problem

The COVID-19 pandemic is a persistent world wide outbreak of COVID-19 brought on by coronavirus 2 associated with severe acute respiratory syndrome. The first case of COVID-19 in Ethiopia was identified on March 13, 2020, in Addis Ababa, the country's capital. There have been 253,120 confirmed cases of COVID-19 and 3,570 deaths in Ethiopia as of April 27, 2021, respectively (WHO, 2020a)

The development of more effective control measures may greatly benefit from the use of mathematical models for COVID-19 infection, which can offer better insights into the dynamics of the virus. The COVID-19 pandemic has been the subject of numerous mathematical

models. Çakan (2020), proposed time delayed SEIR epidemic model with compartments consisting of Susceptible (S) against to the disease COVID-19, Exposed (E), Infectious (I) and Recovered (R) individuals by taking into account the impact of health care capacity. However,the author did not account for the asymptomatic (infectious individuals who do not exhibit disease symptoms) or the immunized (individuals who can receive vaccine). Thus, By incorporating asymptomatic, immunized individuals and applying new mathematical models based on (Çakan, 2020) , we were able to predict the trends of an epidemic with a time delay. Following modeling, the equilibria's stability and existence criteria in terms of the reproduction number is established. The model equation's key parameters were subjected to sensitivity analysis to determine their relative importance and potential influence on the COVID-19 transmission dynamics. The final model parameters proposed are fitted with authentic Ethiopian data.

1.3 Objectives of the study

1.3.1 General objective

The general objective of this study is to formulate a non-linear SVEAIR model to investigate the dynamics of COVID-19 with time delay.

1.3.2 Specific objectives

- Formulate a deterministic SVEAIR mathematical model for COVID-19 transmission dynamics.
- Analyze the qualitative behavior of deterministic SVEAIR mathematical model.
- Formulate a deterministic time delay SVEAIR mathematical model for COVID-19 transmission dynamics.
- Analyze the qualitative behavior of deterministic SVEAIR mathematical model with time delay.

1.4 Significant of the study

A well studied and organized paper report on COVID-19 will provide strong information on how to design appropriate control and preventive measures in order to bring a long term solution. Thus, the outcome of this study are helpful to

- improve decision making at strategical level and adds advantage of interpret the situation of the coronavirus disease,
- propose a strategy for awareness campaigns to target COVID-19 by using time delay model giving more accurate transmission of corona virus,
- motivate other researchers for further study and mathematical analysis.

1.5 Operational Definition of Technical Terms

The following epidemiological terms are defined for later use (M. Y. Li, 2018).
Epidemic is the rapid spread of disease to a large number of people in a given population within a short period of time.
In epidemiology, an infection is said to be **endemic** in a population when that infection is constantly maintained at a base line level in a geographic area without external inputs.
A pandemic is an epidemic of an infectious disease that has spread across a large region, for instance multiple continents or worldwide, affecting a substantial number of people.

1.6 Mathematical Preliminary

In this section, we state some theorems and give the definitions of important concepts for later use in this study. The aim is to clarify terminologies and results that are utilized in the subsequent chapters.

1.6.1 Linearizion and the Jacobian

In most of the systems of real world problem, it becomes apparent that nearly all systems are non-linear, including the model we are examining. However, most of the theory that has been developed by mathematicians governing the behavior of systems of differential equations,

especially stability, is centered upon linear systems. Thus, in order to further understand the behavior of a non-linear system it is first crucial to linearize the system. Essentially, this process approximates a non-linear system in a linear manner near the values around which a linear approximation occurs.

In a neighborhood of the equilibria we can make a linear approximation to determine the system at the equilibria to be determined and provides a starting point for global investigations of solutions. The goal of this stability analysis is to perturb the system from equilibrium and study the behavior of the system. Thus, we will look to see if the solutions move towards or away from equilibrium. In order to linearize the system, we must compute the Jacobian matrix of the system. The Jacobian is the matrix of the partial derivatives of each function with respect to each variable. Essentially, the Jacobian provides a linear approximation of a system at any given value (Layek, 2015).

1.6.2 Routh-Hurwitz Criteria

The linear stability of a system of differential equations:

$$\frac{dX}{dt} = AX$$

Where, $X = (x_1, x_2, ..., x_n)$ is determined by the roots of the characteristic polynomial, A is the Jacobian matrix of the linearized system. The solution of the system is obtained by setting $X = x_0 e^{\lambda t}$. Where x_0 is a constant vector to be determined, λ is the eigenvalue of A. The solution $X = x_0 e^{\lambda t}$ (the equilibrium point) is locally stable if all the roots of the characteristic polynomial:

$$P(\lambda) = \lambda^n + a_1\lambda^{n-1} + a_2\lambda^{n-2} + ... + a_{n-1}\lambda + a_n = 0$$

lie in the left hand complex plane that is $Re(\lambda) < 0$ for all roots λ of characteristic polynomial. Now consider the polynomial

$$\lambda^n + a_1\lambda^{n-1} + a_2\lambda^{n-2} + ... + a_{n-1}\lambda + a_n = 0$$

where all the coefficients $a_1, a_2, ..., a_n$ are real and $a_n \neq 0$. The necessary and sufficient condition for all the roots of the characteristic polynomial equation to have $Re(\lambda) < 0$ is the

Routh-Hurwitz conditions (Merkin, 1997). These Routh-Hurwitz condition are with $a_n > 0$,

$$D_1 = a_1 > 0$$

$$\det(D_2) = \begin{vmatrix} a_1 & 1 \\ a_3 & a_2 \end{vmatrix} = a_1 a_2 - a_3 > 0$$

$$\det(D_3) = \begin{vmatrix} a_1 & 1 & 0 \\ a_3 & a_2 & a_1 \\ 0 & 0 & a_3 \end{vmatrix} = a_1 a_2 a_3 - a_3^2 > 0$$

.

.

.

$$\det(D_n) = \begin{vmatrix} a_1 & a_3 & a_5 & . & . & . \\ 1 & a_2 & a_4 & . & . & . \\ 0 & a_1 & a_3 & . & . & . \\ . & & & & & \\ . & & & & & \\ .0 & 0 & 0 & . & . & . & a_k \end{vmatrix} > 0, \text{for k =1, 2, 3, ... ,n.}$$

1.6.3 Method of Computing Basic Reproduction Number

The basic reproduction number, which is denoted by R_0 is the average number of new cases (infections), that one infected case will generate during its entire infectious life time. The basic reproduction number is an important non-dimensional quantity in epidemiology as it sets the threshold in the study of a disease both for predicting its outbreak and for evaluating its control strategies (Diekmann et al., 1990). Thus, whether a disease becomes persistent or dies out in a community depends on the value of the reproduction number R_0. If $R_0 < 1$ it means that every infectious individual will cause less than one secondary infection which is impossible and hence the disease will die out and when $R_0 > 1$ every infectious individual will cause more than one secondary infection and hence the disease will invade the population. Therefore, the basic reproduction number is a threshold parameter for a disease and its biological significance is obvious. Van den Driessche & Watmough (2002) developed a

technique for calculating the basic reproduction number of disease transmission models. This method is called the next generation operator method. Consider a disease transmission model that has non-negative initial conditions and can be expressed in terms of the following autonomous system:

$$\frac{x_i}{dt} = \mathcal{F}_i(x) - \mathcal{V}_i(x) \tag{1.1}$$

Where $\mathcal{V}_i = \mathcal{V}_i^- + \mathcal{V}_i^+$

- $\mathcal{F}_i(x)$ the rate of appearance of new infections in compartment i,
- $\mathcal{V}_i^+(x)$ the rate of transfer of individuals into compartment i by all others means,
- $\mathcal{V}_i^-(x)$ be the rate of transfer of individuals out of compartment i ,

The functions $\mathcal{F}(x)$, $\mathcal{V}_i^+$, $\mathcal{V}_i^-$ are assumed to be at least twice continuous-differentiable in each variable (Van den Driessche & Watmough, 2002).

1.6.4 Determining the Direction of Bifurcation

Bifurcation is a qualitative changes in the behavior of systems, where one or more system parameters are varied. The study of bifurcation is concerned with how the structural and behavioral change occurs when the parameter (s) are changing. The structural change and the transition behavior of a system are the central part of dynamical evolution. The point at which bifurcation occurs is known as the bifurcation point (Layek, 2015).

For the most part, in epidemic models, there are two distinct bifurcations at $R_0 = 1$ forward (supercritical) and backward (subcritical). A forward bifurcation happens when R_0 crosses unity from below; a small positive asymptotically stable equilibrium appears and the disease-free equilibrium losses its stability. On the other hand, a backward bifurcation happens when R_0 is less than unity; a small positive unstable equilibrium appears while the disease-free equilibrium and a larger positive equilibrium are locally asymptotically stable (Huang et al., 1992). Center manifold theory has been used to decide the local stability of a nonhyperbolic equilibrium (linearization matrix has at least one eigenvalue with zero real part) (Carr, 2012).

Theorem 1. *Castillo-Chavez & Song (2004). Consider the following general system of ordinary differential equations with a parameter* β.

$$\frac{dx}{dt} = f(x, \beta), f : \mathbb{R}^n \times \mathbb{R} \Rightarrow \mathbb{R}^n, f \in C^2(\mathbb{R}^n \times \mathbb{R}) \tag{1.2}$$

Without loss of generality, it is assumed that 0 is an equilibrium point for system (1.2) for all values of the parameter β (that is $f(0, \beta) = 0$) for all β and assume that

$\boldsymbol{A_1} : A = d_x f(0, 0) = \frac{\partial f_i}{\partial x_j}$ is the linearization of system (1.2) around the equilibrium 0 with β evaluated at 0. Zero is a simple eigenvalue of A and all other eigenvalues of A have negative real parts.

$\boldsymbol{A_2}$: Matrix A has a non-negative a right eigenvector w and a left eigenvector v corresponding to the zero eigenvalue.

Let f_k be the k^{th} component of f and

$$\boldsymbol{a} = \sum_{k,i,j=1}^{4} v_k w_i w_j \frac{\partial^2 f_k}{\partial x_i \partial x_j}(0, 0), \boldsymbol{b} = \sum_{k,i=1}^{4} v_k w_i \frac{\partial^2 f_k}{\partial x_i \partial \beta}(0, 0) \tag{1.3}$$

The local dynamic of (1.2) around 0 are totally governed by parameters $\boldsymbol{a}$ and $\boldsymbol{b}$.

1) $\boldsymbol{a} > 0$, $\boldsymbol{b} > 0$, when $\beta < 0$ with $|\beta| < 1$, 0 is locally asymptotically stable, and there exists a positive unstable equilibrium; when $0 < \beta < 1$, 0 is unstable and there exists a negative and locally asymptotically stable equilibrium.

2) $\boldsymbol{a} < 0$, $\boldsymbol{b} < 0$, when $\beta < 0$ with $|\beta| < 1$, 0 is unstable; when $0 < \beta < 1$, 0 is locally asymptotically stable, and there exists a positive unstable equilibrium.

3) $\boldsymbol{a} > 0$, $\boldsymbol{b} < 0$, when $\beta < 0$ with $|\beta| < 1$, 0 is unstable, and there exists a locally asymptotically stable negative equilibrium; when 0 < β < 1, 0 is stable, and a positive unstable equilibrium appears.

4) $\boldsymbol{a} < 0$, $\boldsymbol{b} > 0$, when β changes from negative to positive, 0 changes its stability from stable to unstable. Correspondingly, a negative unstable equilibrium becomes positive and locally asymptotically stable.

1.6.5 Numerical Methods for System of ODEs

Numerical techniques that listed below are summarized from Lenhart & Workman (2007). When a system of ODEs involves equations that can not be solved analytically, numerical

methods are used to compute its approximate solution. For example, fourth order Runge Kutta method $(RK4)$ is widely used for solving initial value problems (IVP) for ordinary differential equation (ODE) which is given

$$\dot{x} = \frac{dx}{dt} = f(t, x),\ x(t_0) = x_0$$

on the interval $t_0 \leq t \leq T$, we divide the interval into N small segments of constant length h, which is called the step size given by $h = \dfrac{T - t_0}{N}$. The numerical methods introduced for a single equation can be easily extended to systems of equations. For example, consider the system of Ordinary differential equation with initial condition.

$$\begin{cases} \dfrac{dx}{dt} = f(t, x, y), & x(t_0) = x_0 \\ \dfrac{dy}{dt} = g(t, x, y), & y(t_0) = y_0 \end{cases} \tag{1.4}$$

We want to obtain a numerical solution on the interval $t_0 \leq t \leq T$. The first step is discretizing the interval by defining the time steps given by

$$t_n = t_0 + nh, \quad n = 0, 1, 2, \cdots N$$

where N is the number of steps. Again we use the notation x_n and y_n to denote the approximate values of $x(t_n)$ and $y(t_n)$, respectively. We can summarize the numerical techniques as:

Runge-Kutta Fourth Order

Given a well-posed initial-value problem (IVP) for the above condition 1.4, the Runge-Kutta method of order four $(RK4)$ constructs a sequence of approximation points $(t, x) \approx (t, x(t))$ and $(t, y) \approx (t, y(t))$ to the exact solution of an ODE by $t_{n+1} = t_n + h$ to get the following values of eight slope:

$$\begin{cases} k_{11} = f(t_n, x_n, y_n) \\ k_{21} = f(t_n, x_n, y_n) \\ k_{12} = f(t_n + \frac{h}{2}, x_n + \frac{h}{2}k_{11}, y_n + \frac{h}{2}k_{21}) \\ k_{22} = f(t_n + \frac{h}{2}, x_n + \frac{h}{2}k_{11}, y_n + \frac{h}{2}k_{21}) \\ k_{13} = f(t_n + \frac{h}{2}, x_n + \frac{h}{2}k_{12}, y_n + \frac{h}{2}k_{22}) \\ k_{23} = f(t_n + \frac{h}{2}, x_n + \frac{h}{2}k_{12}, y_n + \frac{h}{2}k_{22}) \\ k_{14} = f(t_n + h, x_n + hk_{13}, y_n + hk_{23}) \\ k_{24} = f(t_n + h, x_n + hk_{13}, y_n + hk_{23}) \end{cases} \tag{1.5}$$

Then we compute the next approximation using weighted averages of the above slopes,

$$\begin{cases} x_{n+1} = x_n + \frac{h}{6}(k_{11} + 2(k_{12} + k_{13}) + k_{14}) \\ y_{n+1} = y_n + \frac{h}{6}(k_{21} + 2(k_{22} + k_{23}) + k_{24}). \end{cases} \tag{1.6}$$

In such process, the continuous time model is reduced to an approximate discrete time model that is amenable to computer simulation.

1.6.6 Autonomous Linear System

Consider a system of ordinary differential equation which are autonomous.

$$\begin{cases} \frac{dx}{dt} = f(x, y), \\ \frac{dy}{dt} = g(x, y). \end{cases} \tag{1.7}$$

The term autonomous refers to the fact that f and g are not trial function of t .Consider a general autonomous vector field

$$\frac{dx}{dt} = f(x), x \in \mathbb{R}^n \tag{1.8}$$

where $f : \mathbb{R}^n \longrightarrow \mathbb{R}^n$

Definition 1.6.1. *(Layek, 2015) A point $x_e \in \mathbb{R}^n$ is an equilibrium point of the system (1.8) if* $f(x_e) = 0$

To determine the behavior near a critical point, we will linearize the non-linear system around the critical point and use our knowledge of linear systems. Let (x_0, y_0) be the equilibrium point of (1.7). If f and g are n-times continuously differentiable functions, then using the Taylor series expansion.

$$\begin{aligned} f(x,y) =& f(x_0,y_0) + f_x(x_0,y_0)(x-x_0) + f_y(x_0,y_0)(y-y_0) + \frac{1}{2!}f_{xx}(x_0,y_0)(x-x_0)^2 + \\ & \frac{1}{2!}f_{yy}(x_0,y_0)(y-y_0)^2 + f_{xy}(x_0,y_0)(x-x_0)(y-y_0) + \dots \\ \approx& f(x_0,y_0) + f_x(x_0,y_0)(x-x_0) + f_y(x_0,y_0)(y-y_0) \\ =& f_x(x_0,y_0)(x-x_0) + f_y(x_0,y_0)(y-y_0) \end{aligned}$$

$$\begin{aligned} g(x,y) =& g(x_0,y_0) + g_x(x_0,y_0)(x-x_0) + g_y(x_0,y_0)(y-y_0) + \frac{1}{2!}g_{xx}(x_0,y_0)(x-x_0)^2 + \\ & \frac{1}{2!}g_{yy}(x_0,y_0)(y-y_0)^2 + g_{xy}(x_0,y_0)(x-x_0)(y-y_0) + \dots \\ \approx& g(x_0,y_0) + g_x(x_0,y_0)(x-x_0) + g_y(x_0,y_0)(y-y_0) \\ =& g_x(x_0,y_0)(x-x_0) + g_y(x_0,y_0)(y-y_0) \end{aligned}$$

Then, the linearized form of equation (1.7)can be expressed as:

$$\frac{dX}{dt} = AX$$

where $A = \begin{bmatrix} f_x & f_y \\ g_x & g_y \end{bmatrix}$, $x = \begin{bmatrix} x \\ y \end{bmatrix}$ and A is called the Jacobian matrix.

Let $x = ue^{\lambda t}$ be solution of the system of differential equation

$$\frac{dx}{dt} = Ax$$

where u is a vector to determined. Then

$$\frac{dx}{dt} = u\lambda e^{\lambda t} = \lambda x \Longrightarrow Ax = \lambda x \Longrightarrow x(A - \lambda I) = 0.$$

The system will have a non-trival solution if $\det(x(A - \lambda I)) = 0$.

Definition 1.6.2. *(Layek, 2015) A point x_e is said to be stable for a given $\varepsilon > 0$, there exists a $\delta = \delta(\varepsilon) > 0$ such that, for any other solution, $y(t)$ of (1.8) satisfying $|x_e(t_0) - y(t_0)| < \delta$ implies $|x_e(t) - y(t)| < \varepsilon$, for $t > t_0$, $t_0 \in \mathbb{R}$.*

Definition 1.6.3. *(Layek, 2015) A point $x_e(t)$ is said to be locally asymptotically stable if it is Liapunov stable and for any other solution, $y(t)$ of 1.8, there exists a constant $b > 0$ such that if $|x_e(t_0) - y(t_0)| < b$, then $\lim_{t\to\infty}|x_e(t) - y(t)| = 0$.*

Theorem 2. *(Perko, 2013) Let x_0 be a hyperbolic equilibrium point of the nonlinear system 1.8 with $f \in C^1$ (continuously differentiable of order one). Then the stability of the equilibrium point for the nonlinear system is structurally the same as that of the linear system $\dot{x} = Ax$. Where $A = Df(x_0)$.*

A powerful method for analyzing the stability of an equilibrium point is based on the use of Lyapunov functions.

Definition 1.6.4. *Layek (2015) A function V: $\mathbb{R}^n \to \mathbb{R}$ is said to be positive define if,*

- $V(x) > 0$, *for all* $x \neq 0$,
- $V(x) = 0$ *if and only if* $x = 0$,
- $V(x) \to \infty$ *as* $x \to \infty$.

Any function V is called a Lyapunov function, if it satisfies the conditions of positive definite and $\frac{dV}{dt} \leq 0$, $\forall x \in D/\{x_0\}$.

Theorem 3. ***See in (Layek, 2015).*** *Let x_0 be an equilibrium point of the system of (1.8) and consider $V : D \in \mathbb{R}^n \to \mathbb{R}$ be continuously differentiable function such that*

- $V(x_0) = 0$,
- $V(x) > 0\ \forall x \in D \subseteq R^n$,
- $\dfrac{dV}{dt} < 0\ \forall x \in D/\{x_0\}$, $\|x\| \to \infty \Longrightarrow V(x) \to \infty$.

Then the point x_0 is globally asymptotically stable.

Definition 1.6.5. *(Invariant Set) A set E is an invariant set with respect to (1.8) if $x(0) \in E$ implies $x(t) \in E$, $\forall t \in \mathbb{R}_+$ and a set E is positively invariant set with respect to (1.8) if $x(0) \in E$, implies $x(t) \in E$, $\forall t \geq 0$.*

CHAPTER 2

LITERATURE REVIEW

In this chapter, we review some related literature on COVID-19 outbreaks and transmission dynamics that are directly related to the study's objectives. The analysis based on mathematical models greatly aids decision makers in estimating the risk and potential future spread of the disease in the population. Understanding the infection's transmission dynamics is also critical for developing appropriate intervention strategies with low implementation costs. In general, by approaching infectious diseases mathematically, we can identify patterns and common systems in disease function, allowing us to discover some of the underlying structures that govern outbreaks and epidemics, as well as their future trends.

Numerous academics have recently researched various COVID-19 epidemic models. In order to represent the potential for transmission in a specific general population. Zhang (2020) proposed a new mathematical model (SEIRD) that is built with five compartments, including susceptible, exposed, infected, recovered, and dead. They provided a thorough examination of the proposed model, which included the derivation of endemic and disease-free equilibrium points; reproductive number utilizing the next generation matrix; stability analysis of the equilibrium points; and, lastly, the model solutions' positivity. The concept of fractional differentiation was added to the model in order to account for various memory-related characteristics such as power law, decay, and crossover. The numerical solutions for various memories were provided using a Newton-based numerical technique. However, they did not take into account the Vaccinated and Asymptomatic groups. Additionally, their model did not account for time delay.

Bhadauria et al. (2021) studied the SIQ model by using the stability theory of non-linear ordinary differential equations. The basic reproduction number is calculated, and important factors that maintain the basic reproduction number below one are found. According to their research, sickness only leaves the system when a total lockdown is implemented; otherwise, disease would always be present in the population. However, due to its impact on economic crises, the lockdown is challenging to implement in both poor and developed nations. Also excluded from their approach are the classes of Vaccinated, Exposed, Asymptomatic, and Recovered, as well as time delay.

Y. Li & Zhang (2020) developed a numerical method preserving positivity for a stochastic SIQS epidemic model. They create an explicit EM scheme for a stochastic SIQS epidemic model as well as a BIM for a stochastic SIQS epidemic model that preserves positivity. Finally, they demonstrate BIM convergence for the stochastic SIQS epidemic model. Although they did not extend their model to time delay, In addition, the vaccinated, exposed, asymptomatic, and recovery groups are not included in their model. A θ-SEIHQRD model which is more relevant to COVID-19 was developed by Ramos et al. (2021). They carry out a mathematical analysis to demonstrate the system's non-negativity, boundedness, presence of a disease-free equilibrium point, and lack of an endemic equilibrium. On actual data sets from Italy, they test the suggested approach. Finally, they discussed the effects of various control strategies, and the model incorporates people who are hospitalized and under quarantine to calculate the estimated number of beds that are required. The vaccinated and asymptomatic classes are not taken into account in the model, and time delay was not taken into account.

Nisar et al. (2021) constructed the SIRD model and verified its accuracy. In Caputo's sense, they discussed a fractional order SIRD mathematical model of the COVID-19 disease. They used the next generation matrix to arrive at a reproduction number formula. The stability results were computed using basic reproduction numbers. They prove the existence and uniqueness of the solution by using fixed point theory. They also compared their results to some previously published real data on the number of confirmed infection and death cases per day for the first 67 days in Wuhan city. The fact that they neglected to consider the classes of vaccinated, exposed, asymptomatic individuals and time delay. In particular, Paré et al. (2020) investigated conventional group models, continuous-time and discrete-time versions of the models with non-trivial networks on straight forward SIR-based models, and supported the need for networked models by presenting a number of simulations. They proposed a number

of models, including SIS, SIR(S), SEIR(S), and SAIR (S). However, they didn't consider the vaccine compartment and the time delay into account.

At the same time, many researchers analyzed the stability of the COVID-19 model. Araz (2021), dealt with a mathematical model of COVID-19 spread and analyzed global and local stability for the considered model. The author proposed susceptible, asymptomatic infectious, symptomatic infectious unreported, and symptomatic infectious individuals reported by health services. The model is extended to optimal control and numerical simulation is performed to solve the extended model. However the proposed model did not consider the vaccinated classes and the time delay model.

Annas et al. (2020) carried out the stability analysis and numerical simulation of the SEIR model on the spread of COVID-19 in the research. Besides, some scholars conducted mathematical analysis on the principle of COVID-19 infection. They ignored the vaccinated, asymptomatic, and time-delayed groups. Almocera et al. (2021) studied with in-host model, and the stability of a unique positive equilibrium point, with viral load v^*, suggested that the virus may replicate fast enough to overcome T cell response and cause infection. They did not include the vaccinated, asymptomatic, and time delay classes in their model.

Ghostine et al. (2021) proposed an extended SEIR model with a vaccination compartment to simulate the novel coronavirus disease (COVID-19) spreading in Saudi Arabia. Their model considers seven stages of infection: susceptible (S), exposed (E), infectious (I), quarantined(Q), recovered (R), death (D), and vaccinated (V). Initially, they conduct a mathematical analysis to illustrate the non-negativity, boundedness, and epidemic equilibrium; the existence and uniqueness of the endemic equilibrium; and the basic reproduction number of the model. They used an ensemble Kalman filter (EnKF) to constrain the model outputs and its parameters with available data. They apply the proposed assimilation system to real data sets from Saudi Arabia. Finally, they investigate the effect of vaccination on the spread of the pandemic. Hence, they did not consider the asymptomatic classes and the time delay in their model.

In addition, some scholars used the models with several compartments to put forward analysis and opinions on epidemic prevention and control. Carli et al. (2020) proposed a multi-region SIRQTHE model and an optimal control approach, which supported governments in defining the most effective strategies to be adopted during post-lock down mitigation

phases in a multi-region scenario. Giordano et al. (2020) established a SIDARTHE model that predicted the course of the epidemic to help plan an effective control strategy. Odagaki (2021) developed a theoretical frame work based on expected utility theory to find an optimal strategy for minimizing the maximum number of infected people and controlling pandemic spread. Saldaña et al. (2020) developed a compartmental epidemic model of the COVID-19 epidemic outbreak to evaluate the theoretical impact of plausible control interventions. All of them did not consider vaccinated classes and time delays in their models.

Chernet et al. (2020) developed a mathematical model for the transmission dynamics of COVID-19. They considered the SEIAHR model, where the state variables S, E, I, A, H, and R represent susceptible, exposed, symptomatic infected, asymptomatic infected, isolated, or hospitalized and recovered/immune cases, respectively. They have divided the infected cases into two groups: symptomatic and asymptomatic cases. They investigate qualitative analysis including the existence and uniqueness of positive solutions and local and global stability analysis of the disease free and endemic equilibrium points. The result of the sensitivity analysis showed that the most sensitive parameter of the reproductive number is the rate of transmission from asymptotically infected cases to suspected individuals. Despite the fact that they did not account for vaccinated classes or time delays in their model.

In the propagation process of COVID-19, we consider that there is a time delay from exposure to infection . At present, some research has been implemented with a time delay to the epidemic models. By taking into account the time delay effect of infected people during the epidemic's spread, Zhu & Zhu (2021) developed a time delayed reaction diffusion model that is closer to the actual spread of the COVID-19 epidemic. Their model is divided into six compartments, namely susceptible individuals (S), exposed individuals (E), quarantined individuals in their home (H), infected individuals (I), quarantined individuals in hospital(Q) and temporary restorers(R) with time delay. They analyze the model qualitatively and quantitatively with a time delay. Finally, they used real data from USA and China to investigate the numerical solution of the model in various cases, although they did not consider the asymptomatic and vaccinated classes.

Ebraheem et al. (2021) presented a new modified SIR model which incorporates appropriate delay parameters, leading to a more precise prediction of COVID-19 real time data. They propose that the efficacy of the newly developed SIR model is proven by comparing its predictions with real data obtained from four countries, namely Germany, Italy, Kuwait, and

Oman, with epidemic data up to November 26, 2020. The two delay periods for incubation and recovery within the SIR model are proposed and the basic reproduction number R_0 for the given period is estimated. The mathematical analysis of the model in terms of stability analysis is derived and discussed in detail. But the natural death rate, the requirement rate, the COVID-19 death rate, the loss of immunity after recovering from the infection are not considered. Vaccinated, asymptomatic, exposed compartments are not considered, and the delay part is not analyzed in an appropriate way.

Çakan (2020) proposed a time delayed SEIR epidemic model with compartments consisting of Susceptible (S) against the disease COVID-19, Exposed (E) to the corona virus, Infectious (I), and Recovered (R) individuals while considering the impact of health care capacity. The disease-free equilibrium and endemic equilibrium of the model are determined. The local and global stabilities of these equilibria are analyzed by using the corresponding characteristic equation and by using LaSalle's Invariance Principle and Lyapunov's direct method, respectively. They determined the sensitivity analysis and concluded that the disease induced death rate will increase and the recovery rate will decrease while the level of availability to opportunities provided by the healthcare system decreases. Although the paper did not consider the immunity lost after recovering, asymptomatic individuals and vaccine groups.

As mentioned above, all studies developed mathematical models of COVID-19 transmission dynamics by viewing different aspects. But many of them did not consider exposed, vaccinated, asymptomatic, and symptomatic (infected) individuals in one model. Many of them said nothing about the time delay. But from the above review, Chernet et al. (2020) used asymptomatic and symptomatic in one model. Despite the fact that they did not take into account the induced death rate on symptomatic and vaccinated individuals and the time delay in their model, we introduced symptomatic (in this case, there is an induced death rate) and vaccinated individuals in this study to fill the entire gap left by these studies. Next, we extend the model to time delay model.

CHAPTER 3

RESEARCH METHODOLOGY

In this chapter, we described the tools and resources used to accomplish the broad and detailed goals listed in Section 1.3. The study used the following study areas and mathematical techniques.

3.1 Study Area

Ethiopia is located in the Horn of Africa, a region of northern Africa. Addis Ababa serves as the nation of Ethiopia's capital. It has 121279271 people, making it the twelfth most populous nation worldwide and the second most populous country in Africa (behind Nigeria), according to UN data(2022.est). Ethiopians make up 1.47% of the world's population. Its neighbors include Eritrea to the north, Djibouti to the northeast, Somalia to the east, Kenya to the south, and Sudan and South Sudan to the west. Total land area of the nation is 1,104,300 square kilometers WHO (2020a). From 2010–11 to 2019–20, Ethiopia's economy grew strongly and broadly, averaging 9.4% a year. Due to the COVID-19 (cornavirus) pandemic, Ethiopia's real gross domestic product (GDP) growth slowed to 6.1% in 2019–20. Primarily in the construction industry and services made up the majority of the growth. The COVID-19 pandemic had no effect on agriculture, and it contributed slightly more to growth in 2019–20 than it had in 2018–19. Demand-side growth is explained by private consumption and public investment, with the latter playing an increasingly significant role Worldbank (2020).

3.2 Source of Data

The researcher used secondary data and relevant parameters values from literatures in addition to the following:

- reported data on COVID-19 by the Ethiopian Public Health and WHO,
- Books, published journals, and related studies from internet.

3.2.1 Method of Data Analysis

The study involved both qualitative and quantitative analysis. Thus, the data is analyzed using MATLAB software and the results are displayed in the form of tables and figures.

3.3 Descriptions of Mathematical Procedure

We used analytical and numerical methods to accomplish the goal of this research. First, using a set of non-linear ODEs, we created an SVEAIR that described a deterministic dynamical model of COVID-19. A qualitative analysis of the model was done. Linearization and Lyapunov functions, respectively, have been used to analyze the local and global stability of the equilibrium points of the model equations. It has been determined which parameter has a higher impact on the dynamics of COVID-19 infection transmission through sensitivity analysis of the systems. We then used non-linear DDEs to expand the model into a delay deterministic model. A qualitative evaluation of the new model was also done. To supplement the analytical solution of the model, we performed a numerical simulation of the model by using Matlab software(ode45 and dde23).

CHAPTER 4

DETERMINISTIC MATHEMATICAL MODEL FOR COVID-19

This chapter presents a deterministic mathematical model for COVID-19 pandemic using a system of nonlinear ordinary differential equations. Model description and analysis are also detailed in order.

4.1 Model Description and Formulation

In this section, we consider an SVEAIR type mathematical modeling for the dynamics of COVID-19 pandemic. The total population $N(t)$ is divided into six compartments: Susceptible $S(t)$, Vaccinated $V(t)$, Exposed $E(t)$, Asymptomatic A(t), Infected $I(t)$ and Recovered $R(t)$ population at time $t \geq 0$. Thus, total population is given by

$$N(t) = S(t) + V(t) + E(t) + A(t) + I(t) + R(t)$$

The description of all the state variables are given in Table 4.1.
The model assumed that susceptible individuals are recruited (by birth or immigration) into the population at a constant rate Λ. A proportion of the susceptible individuals become exposed to the COVID-19 infection at a rate $\lambda = \frac{\beta(I+qA)}{N}$ which is called force of infection as given in (Gurmu et al., 2020) when they come in to effective contact with an infectious individuals at a rate β, where β is an effective contact rate and q is the transmission coefficient for the asymptomatic individuals. In the model, κ is a per capita rate of becoming infectious. A proportion of ρ of the individuals in the compartment E may develop a symptoms of the

Table 4.1: Notations and description of the model variables

Variable	Description
$S(t)$	Susceptible populations which are vulnerable to the disease at time t,
$V(t)$	Individuals who have been vaccinated
$E(t)$	The number of individuals who are exposed but are not yet infectious at time t,
$A(t)$	Infectious individuals who are not show symptoms of the disease at time t,
$I(t)$	Infectious individuals who are not show symptoms of the disease at time t,
$R(t)$	Individuals who have been recovered from the infection at time t,
$N(t)$	Total population at time t,

COVID-19 infection and move to the infected compartment I at a rate $\kappa\rho$. The rest of individuals becomes asymptomatic with COVID-19 infection with probability $(1-\rho)$ and move to the class A at a rate $\kappa(1-\rho)$. Furthermore, an individual in asymptomatic A compartement is recovered due to natural immunity and move to recovered class R at a rate γ. The infected individuals I recovered after receiving a treatment at a rate α and move to the recovered class R. A recovered individuals may revert to the susceptible class S after losing their immunity at a rate θ. Compared to the model introduced in (Çakan, 2020), the present model differ due to presence of vaccinated individual and consideration of asymptomatic compartment. Besides, we assumed that the portion of recovered populations are re-susceptible due to immunity lose. All individuals in $N(t)$ suffers natural mortality at a rate μ. In addition to these model description, the formulation of the governed mathematical model is based on the following assumptions: the size of population is constant, natural birth rate and death rate are not equal, all parameters are non-negative, all individuals in the community are susceptible when there is no disease. The corresponding COVID-19 transmission diagram is depicted in figure 4.1.

The compartmental epidemic system for COVID-19 is governed by the system of non-linear ordinary differential equations:

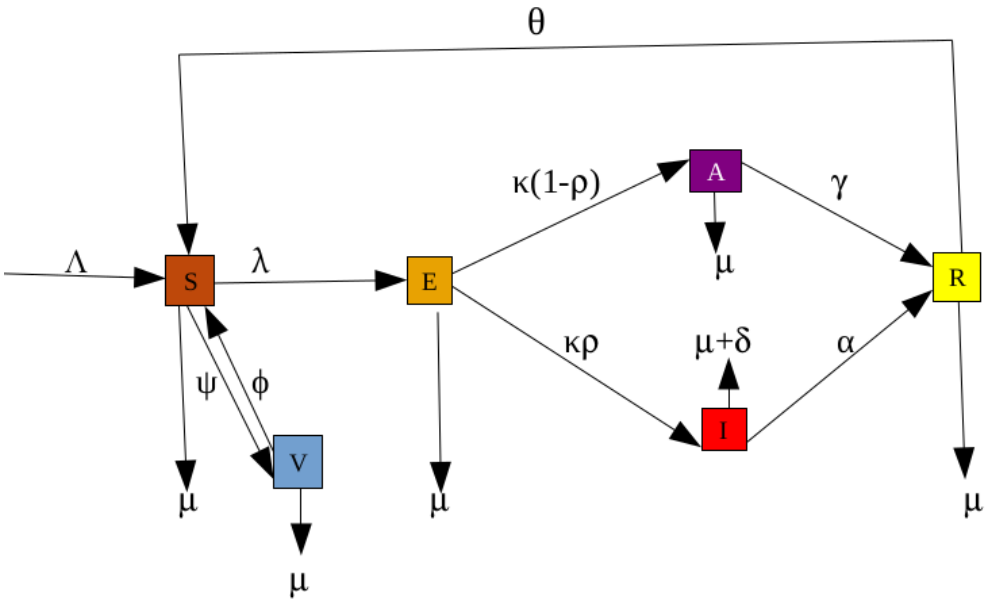

Figure 4.1: Compartmental flow diagram for COVID-19 transmission.

$$
\begin{aligned}
\frac{dS(t)}{dt} &= \Lambda + \theta R(t) + \phi V(t) - \lambda S(t) - \psi S(t) - \mu S(t),\\
\frac{dV(t)}{dt} &= \psi S(t) - \phi V(t) - \mu V(t),\\
\frac{dE(t)}{dt} &= \lambda S(t) - (\kappa + \mu) E(t),\\
\frac{dA(t)}{dt} &= \kappa(1-\rho) E(t) - (\gamma + \mu) A(t),\\
\frac{dI(t)}{dt} &= \kappa\rho E(t) - (\alpha + \delta + \mu) I(t),\\
\frac{dR(t)}{dt} &= \gamma A(t) + \alpha I(t) - (\theta + \mu) R(t).
\end{aligned}
\tag{4.1}
$$

where $\lambda = \frac{\beta(I+qA)}{N}$. The non-negative initial conditions are given as $S(0) > 0$, $V(0) \geq 0$, $E(0) \geq 0$, $A(0) \geq 0$, $I(0) \geq 0$, $R(0) \geq 0$. The parameter descriptions are also given in Table 4.2.

Table 4.2: Description of model parameters and values for later use.

Parameter	Description	value	Reference
Λ	Recruitment rate	5994(per day)	Estimated
β	Effective contact rate of infection	0.92	fitted
κ	Per capita rate of becoming infectious	0.1249	fitted
q	Transmission rate for asymptomatic individuals	0.4722	fitted
ρ	Probability of exposed individuals joining infectious class	0.9692	fitted
α	Progression from compartment $I(t)$ to $R(t)$ due to effective treatment	0.5001(per day)	fitted
δ	Death rate due to disease in the symptomatic compartment	0.00021(per day)	fitted
ϕ	The rate vaccine wanes	0.4231(per day)	fitted
ψ	The transmission rate of susceptible into vaccinated class	0.0891(per day)	fitted
γ	Rate at which asymptomatic individuals recovered	0.2970(per day)	fitted
μ	Natural death rate	0.0000494266(per day)	fitted
θ	Rate at which recovered individuals reverts to susceptible class	0.00124 per day	fitted

4.2 Model Analysis

4.2.1 Invariant Region

Let us determine a region in which the solution of model (4.1) is bounded. For this model the total population in to time t is given by $N(t) = S(t) + V(t) + E(t) + A(t) + I(t) + R(t)$. Then, differentiating N with respect to time we obtain:

$$\frac{dN(t)}{dt} = \frac{S(t)}{dt} + \frac{dV(t)}{dt} + \frac{dE(t)}{dt} + \frac{dA}{dt} + \frac{I(t)}{dt} + \frac{dR(t)}{dt} = \Lambda - \delta I(t) - \mu N(t)$$

If there is no death due to the disease, we get

$$\begin{aligned} \frac{dN(t)}{dt} &\leq \Lambda - \mu N \\ N'(t) + \mu N(t) &\leq \Lambda. \end{aligned} \tag{4.2}$$

By the method of integrating factor,

$$\frac{d(N(t)e^{\mu t})}{dt} \leq \Lambda e^{\mu t}. \tag{4.3}$$

Integrating both sides of the equation (4.3) and simplifying it, then we have

$$N(t) \leq \frac{\Lambda}{\mu} + ce^{-\mu t}. \tag{4.4}$$

As $t \longrightarrow \infty$ in equation (4.4), the population size $N(t) \longrightarrow \frac{\Lambda}{\mu}$, which implies that $0 \leq N(t) \leq \frac{\Lambda}{\mu}$. Thus the feasible region of the system (4.1) is given by the set

$$\Omega = \left\{(S, V, E, A, I, R) \in \mathbb{R}^6_+ : 0 \leq N(t) \leq \frac{\Lambda}{\mu}\right\} \tag{4.5}$$

is positively invariant. That is,
$\frac{dS}{dt}|_{S=0} = \Lambda+\theta R+\phi V > 0$, $\frac{dV}{dt}|_{v=0} = \psi S \geq 0$, $\frac{dE}{dt}|_{E=0} = \lambda S \geq 0$, $\frac{dA}{dt}|_{A=0} = \kappa(1-\rho)E \geq 0$, $\frac{dI}{dt}|_{I=0} = \kappa\rho E(t) \geq 0$, $\frac{dR}{dt}|_{R=0} = \gamma A + \alpha I(t) \geq 0$.
Consequently, this region attracts all solutions of the system and this restricted region will be enough to consider of the dynamics of the model (4.1).

4.2.2 Existence and Uniqueness of the Solution

The validity and authenticity of any mathematical model depends on the existence and uniqueness of the solutions for the governing system of equations.

Theorem 4. *Let $t > 0$ and the initial conditions satisfies $S(0) > 0$, $V(0) \geq 0$, $E(0) \geq 0$, $A(0) \geq 0$, $I(0) \geq 0$, $R(0) \geq 0$ in the prescribed region Ω. Then the solution of the model system (4.1) exists and unique in $\mathbb{R}^6_+$.*

Proof. The right hand side of the model equation (4.1) can be expressed as follows:

$$\begin{aligned}
f_1(S, V, E, A, I, R) &= \Lambda + \theta R(t) + \phi V(t) - \lambda S(t) - (\psi + \mu)S(t),\\
f_2(S, V, E, A, I, R) &= \psi S(t) - (\phi + \mu)V(t),\\
f_3(S, V, E, A, I, R) &= \lambda S(t) - (\kappa + \mu)E(t),\\
f_4(S, V, E, A, I, R) &= \kappa(1 - \rho)E(t) - (\gamma + \mu)A(t),\\
f_5(S, V, E, A, I, R) &= \kappa\rho E(t) - (\alpha + \delta + \mu)I(t),\\
f_6(S, V, E, A, I, R) &= \gamma A(t) + \alpha I(t) - (\theta + \mu)R(t).
\end{aligned}$$

In the region $\Omega = \left\{(S, V, E, A, I, R) \in \mathbb{R}^6_+ : N(t) \leq \frac{\Lambda}{\mu}\right\}$, the equations (4.1) have a unique solution if $\frac{\partial f_i}{\partial x_j}$, $i, j = 1, 2, ..., 6$, are continuous and bounded in Ω. Here, using notations

$x_1 = S$, $x_2 = V$, $x_3 = E$, $x_4 = A$, $x_5 = I$, $x_6 = R$. When we differentiate the system $\frac{\partial f_i}{\partial x_j}$ it is continuous and bounded in Ω. Here, we observe that f has a continuous first partial derivative with respect to each state variables in $\mathbb{R}^6_+$. It follows that f is locally Lipschitz. Thus, the result is the direct outcome of fundamental existence and uniqueness theorem (Perko, 2013) in $\mathbb{R}^6_+$. □

4.2.3 Non-negativity of Solutions

Theorem 5. *If $S(0) > 0$, $V(0) \geq 0$, $E(0) \geq 0$, $A(0) \geq 0$, $I(0) \geq 0$, $R(0) \geq 0$ are all non-negative, then the solutions $S(t), E(t), A(t), I(t), and\ R(t)$ are all positive for $t > 0$.*

Proof. From the system of differential equation (4.1), let us take the first equation:
$\frac{dS(t)}{dt} = \Lambda + \theta R(t) + \phi V(t) - \lambda S(t) - \psi S(t) - \mu S(t)$,
This equation can be expressed without loss of generality, after eliminating the positive term $(\Lambda + \theta R + \phi V)$, as an inequality

$$\frac{dS}{dt} > -(\frac{\beta(I + qA)}{N} + \psi + \mu)S,$$

Then using separable method of variables and applying integration, the solution of the deferentially inequality can be obtained as

$$S(t) > S(0)e^{-\psi t - \mu t - \int_0^t \frac{\beta(I+qA)}{N} dt} \geq 0.$$

Where $S(0)$ is obtain from initial condition. Since exponential function is always non-negative, the function $e^{-\psi t - \mu t - \int_0^t \frac{\beta(I+qA)}{N} dt}$ is non-negative quantity. Hence, we conclude that $S(t) > 0$. Similarly, the second equation for the system (4.1) is given by

$$\frac{dV(t)}{dt} = \psi S(t) - (\phi + \mu)V(t),$$

After eliminating the positive term $\psi S(t)$ as an inequality as

$$\frac{dV(t)}{dt} \geq -(\phi + \mu)V,$$

Using separable method of variables and on applying integration, the solution of the fore

going differential inequality can be obtained as

$$V(t) \geq V(0)e^{-(\phi+\mu)t},$$

Where $V(0)$ is obtain from initial condition. Recall that an exponential function is always non-negative irrespective of the sign of the exponent, i.e, the exponential function $e^{-(\phi+\mu)t}$ is non-negative quantity. Hence, we can conclude that $V(t) \geq 0$. Similarly, we obtain

$$\begin{aligned} E(t) &\geq E(0)e^{-(\kappa+\mu)t}, \\ A(t) &\geq A(0)e^{-(\gamma+\mu)t}, \\ I(t) &\geq I(0)e^{-(\alpha+\delta+\mu)t}, \\ R(t) &\geq R(0)e^{-(\theta+\mu)t}. \end{aligned}$$

This proves that the solution of system (4.1) are positive for all $t \geq 0$. □

4.2.4 COVID Free Equilibrium Point(CFE)

COVID free equilibrium points is steady state solution where there is no COVID-19 infection. That is, all the infected classes are zero and the entire population comprise of only susceptible and vaccinated individuals. To find the COVID free equilibrium (CFE), we equate the left hand side of the system (4.1) equal to zero at $E(t) = 0$, $I(t) = 0$ and $A(t) = 0$. We denote disease free equilibrium point by E_0. We have that;

$$\begin{cases} \frac{dS(t)}{dt} = \Lambda + \theta R(t) + \phi V(t) - \lambda S(t) - (\psi + \mu)S(t) = 0, \\ \frac{dV(t)}{dt} = \psi S(t) - (\phi + \mu)V(t) = 0, \\ \frac{dE(t)}{dt} = \lambda S(t) - (\kappa + \mu)E(t) = 0, \\ \frac{dA(t)}{dt} = \kappa(1-\rho)E(t) - (\gamma + \mu)A(t) = 0, \\ \frac{dI(t)}{dt} = \kappa\rho E(t) - (\alpha + \delta + \mu))I(t) = 0, \\ \frac{dR(t)}{dt} = \gamma A(t) + \alpha I(t) - (\theta + \mu)R(t) = 0. \end{cases}$$

Solving for the non-infected state variable we obtain the disease free equilibrium point $E_0 = \left(\frac{\Lambda(\phi+\mu)}{\mu(\psi+\phi+\mu)}, \frac{\psi\Lambda}{\mu(\psi+\phi+\mu)}, 0, 0, 0, 0\right)$

4.2.5 The Basic Reproduction Number

In this section, we determine the basic reproduction number. We use the next generation method given in (Van den Driessche & Watmough, 2002) to compute R_0. It is obtained by taking the largest (dominant) eigenvalue (spectral radius).

$$R_0 = \rho(FV^{-1})$$

Next, we derive an expression for the basic reproduction number using the method of the next generation matrix. The first step is rewrite the model equations, starting with newly infective classes

$$\begin{aligned} \frac{dE(t)}{dt} &= \lambda S(t) - (\kappa + \mu)E(t), \\ \frac{dA(t)}{dt} &= \kappa(1-\rho)E(t) - (\gamma + \mu)A(t), \\ \frac{dI(t)}{dt} &= \kappa\rho E(t) - (\alpha + \delta + \mu)I(t), \end{aligned} \tag{4.6}$$

For this model, the associated matrices $\mathcal{F}$ and $\mathcal{V}$ the new infectious terms and the remaining transition terms are respectively given by:

$$\mathcal{F}_i(x) = \begin{bmatrix} \frac{\beta(I+qA)}{N}S \\ 0 \\ 0 \end{bmatrix} \text{ and } \mathcal{V}_i(x) = \begin{bmatrix} (\kappa+\mu)E \\ (\gamma+\mu)A(t) - \kappa(1-\rho)E(t) \\ (\alpha+\delta+\mu)I(t) - \kappa\rho E(t) \end{bmatrix}$$

The Jacobian matrices at the disease-free equilibrium point of $\mathcal{F}$ and $\mathcal{V}$ are obtained by derivating with respect to E, A and I as following:

$$F(E_0) = \begin{bmatrix} 0 & \frac{\beta q(\phi+\mu)}{\psi+\phi+\mu} & \frac{\beta(\phi+\mu)}{\psi+\phi+\mu} \\ 0 & 0 & 0 \\ 0 & 0 & 0 \end{bmatrix} \text{ and } V(E_0) = \begin{bmatrix} \kappa+\mu & 0 & 0 \\ -\kappa(1-\rho) & \gamma+\mu & 0 \\ -\kappa\rho & 0 & \alpha+\delta+\mu \end{bmatrix},$$

$$|V(E_0)| = \begin{vmatrix} \kappa+\mu & 0 & 0 \\ -\kappa(1-\rho) & \gamma+\mu & 0 \\ -\kappa\rho & 0 & \alpha+\delta+\mu \end{vmatrix} = (\kappa+\mu)(\gamma+\mu)(\alpha+\delta+\mu) \neq 0.$$

Hence, the matrix $V(E_0)$ is invertible and thus,

$$V(E_0)^{-1} = \begin{pmatrix} \frac{1}{\kappa+\mu} & o & 0 \\ \frac{\kappa(1-\rho)}{(\kappa+\mu)(\gamma+\mu)} & \frac{1}{\gamma+\mu} & 0 \\ \frac{\kappa\rho}{(\kappa+\mu)(\mu+\alpha+\delta)} & 0 & \frac{1}{\mu+\delta+\alpha} \end{pmatrix} \tag{4.7}$$

Moreover,

$$F(E_0)V(E_0)^{-1} = \begin{pmatrix} \frac{\beta q f \kappa(1-\rho)}{acg} + \frac{\beta\kappa\rho f}{gec} & \frac{\beta q f}{ga} & \frac{\beta f}{ge} \\ 0 & 0 & 0 \\ 0 & 0 & 0 \end{pmatrix} \tag{4.8}$$

Since F is non-negative and V is non-singular, then V^{-1} and FV^{-1} are non negative. The matrix $F(E_0)\,V(E_0)^{-1}$ is called next generation matrix for the model. The eigenvalues of the matrix $F(E_0)\,V(E_0)^{-1}$ can be compute as $det(F(E_0)V(E_0)^{-1} - \lambda I) = |F(E_0)V(E_0)^{-1} - \lambda I| = 0$. Equivalently,

$$|F(E_0)V(E_0)^{-1} - \lambda I| = \begin{vmatrix} \frac{\beta q f \kappa(1-\rho)}{acg} + \frac{\beta\kappa p f}{gae} - \lambda & \frac{\beta q f}{ga} & \frac{\beta f}{ge} \\ 0 & 0-\lambda & 0 \\ 0 & 0 & 0-\lambda \end{vmatrix} = 0 \tag{4.9}$$

where $c = \kappa + \mu$, $a = \gamma + \mu$, $e = \alpha + \delta + \mu$, $f = \phi + \mu$, $g = \psi + \phi + \mu$.

After simple manipulation, the eigenvalues are:

$\lambda_1 = 0$, $\lambda_2 = 0$, $\lambda_3 = \frac{\beta q f \kappa(1-\rho)}{acg} + \frac{\beta\kappa\rho f}{gce}$.

Finally, the basic reproductive number is given by $R_0 = \rho(FV^{-1})$ where $\rho(FV^{-1})$ denotes the spectral radius of the matrix FV^{-1} which is the largest non-negative eigenvalue of the next generation matrix. Therefore,

$R_0 = \lambda_3 = \frac{\beta q f \kappa e(1-\rho)+\beta\kappa\rho a f}{gaec} = \frac{\beta q(\alpha+\mu+\delta)\kappa(1-\rho)(\phi+\mu)+\beta\kappa\rho(\gamma+\mu)(\phi+\mu)}{(\gamma+\mu)(\kappa+\mu)(\mu+\alpha+\delta)(\phi+\psi+\mu)}$.

4.2.6 Endemic Equilibrium Point

The endemic equilibrium point which denoted by E_1 is a steady state solution where the disease persists in the population. The endemic equilibrium $E_1 = (S^*, V^*, E^*, A^*, I^*, R^*)$ can be obtained by equating the left hand side of (4.1) with zero. That means

$$\begin{cases} \Lambda + \theta R^* + \phi V^* - \lambda S^* - (\psi + \mu)S^* = 0, \\ \psi S^* - (\phi + \mu)V^* = 0, \\ \lambda S^* - (\kappa + \mu)E^* = 0, \\ \kappa(1-\rho)E^* - (\gamma + \mu)A^* = 0, \\ \kappa\rho E^* - (\alpha + \delta + \mu)I^* = 0, \\ \gamma A^* + \alpha I^* - (\theta + \mu)R^* = 0. \end{cases}$$

From the above system we can get the values of endemic equilibrium point.

$$S^* = \frac{(\kappa + \mu)E^*}{\lambda} = \frac{aN^*E^*}{\beta(qA^* + I^*)} = \frac{N^*f}{R_0 g}, \tag{4.10}$$

$$V^* = \frac{\psi S^*}{\phi + \mu} = \frac{\psi N^*}{R_0 g}, \tag{4.11}$$

$$A^* = \frac{(1-\rho)\kappa E^*}{a}, \tag{4.12}$$

$$I^* = \frac{\kappa\rho E^*}{e}, \tag{4.13}$$

$$R^* = \frac{\gamma\kappa e(1-\rho) + \alpha\kappa\rho a}{aem} E^*, \tag{4.14}$$

where $\lambda = \frac{\beta(I^* + qA^*)}{N^*}$, $c = \kappa + \mu$, $a = \gamma + \mu$, $e = \alpha + \mu + \delta$, $m = \theta + \mu$, $f = \phi + \mu$, $g = \psi + \phi + \mu$.

Solving for E^* by inserting (4.10), (4.11), (4.12) and (4.14) in to $\Lambda + \theta R^* + \phi V^* - \lambda S^* - \psi S^* - \mu S^* = 0$, we get

$$E^* = \frac{aem\Lambda}{caem - \theta\gamma e\kappa(1-\rho) - \alpha\theta a\kappa\rho)}(1 - \frac{1}{R_0}). \tag{4.15}$$

From (4.12) we can obtain the value of A^*,

$$A^* = \frac{\kappa(1-\rho)em\Lambda}{caem - \theta\gamma e\kappa(1-\rho) - \alpha\theta a\kappa\rho)}(1 - \frac{1}{R_0}).$$

From (4.13) we can determine the values of I^*,

$$I^* = \frac{am\Lambda\kappa\rho}{caem - \theta\gamma e\kappa(1-\rho) - \alpha\theta a\kappa\rho)}(1 - \frac{1}{R_0}).$$

The values of R^* is obtained as follows

$$R^* = \frac{\Lambda(\gamma e\kappa(1-\rho) + \alpha a\kappa\rho)}{caem - \theta\gamma e\kappa(1-\rho) - \alpha\theta a\kappa\rho)}(1 - \frac{1}{R_0}).$$

4.3 Stability Analysis of COVID Free Equilibrium Point

4.3.1 Local Stability of COVID Free Equilibrium Point

Theorem 6. *The disease-free equilibrium* $E_0 = \left(\frac{\Lambda(\phi+\mu)}{\mu(\phi+\psi+\mu)}, \frac{\psi\Lambda}{\mu(\phi+\psi+\mu}, 0, 0, 0, 0\right)$ *of the system (4.1) is locally asymptotically stable if* $R_0 < 1$.

Proof. The Jacobian matrix at the disease-free equilibrium E_0 of the system (4.1) is

$$J(E_0) = \begin{bmatrix} -n & \phi & 0 & \frac{-\beta qf}{g} & \frac{-\beta f}{g} & \theta \\ \psi & -f & 0 & 0 & 0 & 0 \\ 0 & 0 & -c & \frac{\beta qf}{g} & \frac{\beta f}{g} & 0 \\ 0 & 0 & \kappa(1-\mu) & -a & 0 & 0 \\ 0 & 0 & \kappa\rho & 0 & -e & 0 \\ 0 & 0 & 0 & \gamma & \alpha & -m \end{bmatrix} \tag{4.16}$$

Where; $c = \kappa + \mu,\ e = \alpha + \mu + \delta,\ \ a = \gamma + \mu,\ n = \psi + \mu,\ m = \theta + \mu,\ \ f = \phi + \mu,\ g = \psi + \phi + \mu$. The eigenvalues of $J(E_0)$ are the solutions of the characteristics equation $det[J(E_0) - \lambda I_6] = 0$, where I_6 is an identity matrix of order 6. Then we have

$$|J(E_0) - \lambda I_6| = \begin{vmatrix} -n-\lambda & \phi & 0 & \frac{-\beta qf}{g} & \frac{-\beta f}{g} & \theta \\ \psi & -f-\lambda & 0 & 0 & 0 & 0 \\ 0 & 0 & -c-\lambda & \frac{\beta qf}{g} & \frac{\beta f}{g} & 0 \\ 0 & 0 & \kappa(1-\rho) & -a-\lambda & 0 & 0 \\ 0 & 0 & \kappa\rho & 0 & -e-\lambda & 0 \\ 0 & 0 & 0 & \gamma & \alpha & -m-\lambda \end{vmatrix} = 0$$

The corresponding characteristic equation has the following form:

$$(-n-\lambda)(-f-\lambda)[(-c-\lambda)(-a-\lambda)(-e-\lambda)(-m-\lambda)+\frac{\beta q f\kappa(1-\rho)(e+\lambda)(-m-\lambda)}{g}+\frac{\beta f\kappa\rho(a+\lambda)(-m-\lambda)}{g}]-\psi\phi[(-c-\lambda)(-a-\lambda)(-e-\lambda)(-m-\lambda)+\frac{\beta q f\kappa(1-\rho)(e+\lambda)(-m-\lambda)}{g}+\frac{\beta\kappa\rho f(a+\lambda)(-m-\lambda)}{g}]=0 \tag{4.17}$$

Then solving equation (4.17) we obtain

$$-m-\lambda=0,(-n-\lambda)(-f-\lambda)-\psi\phi=0,(-c-\lambda)(-a-\lambda)(-e-\lambda)+\frac{\beta q f\kappa(1-\rho)(e+\lambda)}{g}+\frac{\beta f\kappa\rho(a+\lambda)}{g}=0, \tag{4.18}$$

Clearly, the sign of the first eigenvalue $\lambda_1 = -m$ is negative. To determine the value of the other eigenvalues

$$(-n-\lambda)(-f-\lambda)-\psi\phi=\lambda^2+(n+f)\lambda+nf-\psi\phi=0,$$
$$\lambda_2=\frac{-n-f-\sqrt{(n+f)^2-4dg}}{2},\lambda_3=\frac{-n-f+\sqrt{(n+f)^2-4dg}}{2}.$$

The eigenvalue of λ_2 and λ_3 are negative because of $dg > 0$. To determine the sign of the remaining eigenvalues we use the Routh-Hurwitz criteria which state that the roots of the characteristic equation; $\lambda^3+(e+c+a)\lambda^2+(ec+ae+ac-\frac{\beta f\kappa(q(1-\rho)+p)}{g})\lambda+ace(1-R_0)=0$ are real distinct and negative if the coefficients satisfy the conditions $e+c+a>0, ec+ac+ae-\frac{\beta f\kappa(q(1-\rho)+\rho)}{g}>0, ace(1-R_0)>0$ and $(e+c+a)(ec+ae+ac-\frac{\beta f\kappa(q(1-\rho)+\rho)}{g})-ace(1-R_0)>0$. Here $e+c+a>0$ since all parameters are positive. Again $ec+ac+ae>\frac{\beta f\kappa(q(1-\rho)+\rho)}{g}$ and $ace(1-R_0)>0 \implies R_0<1$. Furthermore,
$(e+c+a)(ec+ae+ac-\frac{\beta f\kappa(q(1-\rho)+\rho)}{g})>ace(1-R_0)$, if $R_0<1$.
Therefore, we can conclude that the disease free equilibrium point of the model equation (4.1) is locally asymptotically stable if $R_0 < 1$. □

4.3.2 Global Stability of the COVID Free Equilibrium Point

Theorem 7. *The disease free equilibrium of the system (4.1) is globally asymptotically stable if* $R_0 < 1$.

Proof. Let $\Omega \subseteq \mathbb{R}^6_+$ be an open neighborhood of the disease free equilibrium point E_0 Then

define the Lyapunove function L, defined by:

$$L = B_1E + B_2A + B_3I \tag{4.19}$$

where B_i, for $i = 1, 2, 3$ are some positive constants. The Lyapunov function L is continuously differentiable as the functions of E, A, I and $L(E_0) = 0$ as well as $L > 0$, $\forall (S, V, E, A, I, R) \in \mathbb{R}^6_+ - \{E_0\}$. Now differentiating L with respect to time we obtain

$$\begin{aligned}
\frac{dL}{dt} &= B_1\frac{dE}{dt} + B_2\frac{dA}{dt} + B_3\frac{dI}{dt} \\
&= B_1(\frac{\beta(I+qA)}{N}S - cE) + B_2(\kappa(1-\rho)E - aA) + B_3(\kappa\rho E - e)I \\
&\leq B_1(\frac{\beta f(I+qA)}{g} - cE) + B_2(\kappa(1-\rho)E - aA)) + B_3(\kappa\rho E - e)I, \ since \ \frac{S}{N} \leq \frac{f}{g} \\
&= (B_2\kappa(1-\rho) - B_1(\kappa+\mu) + B_3\kappa\rho)E + (\frac{\beta B_1 qf}{g} - aB_2)A + (\frac{\beta B_1 f}{g} - B_3)I \\
&= B_1c(\frac{B_2\kappa(1-\rho) + B_3\kappa\rho}{B_1c} - 1)E + (\frac{\beta B_1 qf}{g} - aB_2)A + (\frac{\beta B_1 f}{g} - B_3e)I
\end{aligned}$$

Now choosing $B_1 = gea, B_2 = \beta qef, B_3 = \beta af$; then we have

$$\begin{aligned}
\frac{dL}{dt} &\leq geca(\frac{\beta qef\kappa(1-\rho) + \beta af\kappa\rho}{geac} - 1)E + (\beta eaqf - a\beta qef)A + (\beta eaf - \beta afe)I \\
&= geca(\frac{\beta qef\kappa(1-\rho) + \beta af\kappa\rho}{geac} - 1)E + 0.
\end{aligned}$$

This implies that $\frac{dL}{dt} \leq geca(R_0 - 1)E$. Hence, $\frac{dL}{dt} \leq 0$ For $R_0 \leq 1$ and $\frac{dL}{dt} = 0$ if and only if $E = 0$. Therefore, the largest compact invariant set in Ω is the singleton set $\left(\frac{\Lambda(\phi+\mu)}{\mu(\phi+\psi+\mu)}, \frac{\psi\Lambda}{\mu(\phi+\psi+\mu)}, 0, 0, 0, 0\right)$. Hence, by LaSalle's invariant principle (La Salle, 1976), every solution to equations of model (4.1) with initial conditions in Ω which approaches the disease-free equilibrium point as time t tends to infinity whenever $R_0 < 1$. This implies that the disease-free equilibrium is globally asymptotically stable in Ω. □

4.4 Stability Analysis of Endemic Equilibrium Point

The endemic equilibrium point denoted by $E_1 = (S^*, V^*, E^*, A^*, I^*, R^*)$ is a steady state solution where the disease persists in the population. It is determined above by setting rates of changes of variables with respect to time in the model equation (4.1) to zero.

4.4.1 Local Stability of Endemic Equilibrium Point (EEP)

Theorem 8. *The Endemic equilibrium Point (EEP) of system (4.1) at E_1 is locally asymptotically stable if $R_0 < 1$.*

Proof. To proof the local stability of endemic equilibrium point of the system (4.1) we use linearization approach. Thus, the Jacobian $J(E_1)$ matrix at the endemic equilibrium point becomes

$$J(E_1) = \begin{bmatrix} -n & \phi & 0 & \frac{-\beta q f}{R_0 g} & \frac{-\beta f}{R_0 g} & \theta \\ \psi & -f & 0 & 0 & 0 & 0 \\ u & 0 & -c & \frac{\beta q f}{R_0 g} & \frac{\beta f}{R_0 g} & 0 \\ 0 & 0 & \kappa(1-\rho) & -a & 0 & 0 \\ 0 & 0 & \kappa\rho & 0 & -e & 0 \\ 0 & 0 & 0 & \gamma & \alpha & -m \end{bmatrix} \tag{4.20}$$

where $u = \frac{\beta(qA^*+I^*)}{N^*}$, $c = k+\mu$, $a = \gamma+\mu$, $f = \phi+\mu$, $n = u+\psi+\mu$, $m = \theta+\mu$, $e = \mu+\alpha+\delta$, $g = \phi+\psi+\mu$. The characteristic equation of the Jacobian matrix (4.20) at the endemic equilibrium point is also given by:

$$P(\lambda) = \lambda^6 + A_1\lambda^5 + A_2\lambda^4 + A_3\lambda^3 + A_4\lambda^2 + A_5\lambda + A_6 \tag{4.21}$$

Where;

$A_1 = c_1 + m + c_3,$

$A_2 = c_2 + mc_1 + c_1c_3 + mc_3 + c_4,$

$A_3 = mc_2 + c_3c_2 + mc_3c_1 + c_4c_1 + mc_4 + \dfrac{\beta u f(q\kappa(1-\rho)+\kappa\rho)}{R_0 g},$

$A_4 = mc_3c_2 + c_4c_2 + mc_4c_1 + c_4c_1 + \dfrac{uf(\beta q f\kappa(1-\rho)+\beta\kappa\rho f)}{R_0 g} + \dfrac{\beta m f u(q\kappa(1-\rho)+\kappa\rho)}{R_0 g} -$

$\theta\gamma\kappa(1-\rho)u - \theta\alpha\kappa\rho u,$

$A_5 = mc_2c_4 + \dfrac{\beta m f^2 u(q\kappa(1-\rho)+\kappa\rho)}{R_0 g} + acemu - \theta\gamma\kappa f u(1-\mu) - \theta\kappa\rho f u\alpha -$

$\theta\gamma\kappa(1-\rho)eu - \theta\kappa\rho a\alpha u,$

$A_6 = acemfu - \theta\gamma\kappa(1-\rho)efu - \theta\kappa\rho fa\alpha u.$

$c_1 = n+f,\ c_2 = \phi u + \phi\mu + u\mu + \psi\mu + \mu^2,\ c_3 = a+c+e,\ c_4 = ae + ce + \dfrac{\beta f\kappa(q(1-\rho)+\rho)}{R_0 g},\ u = \lambda$

Here, $u = \beta\frac{(I+qA)}{N^*} = \frac{aecm(bR_0+\delta\psi-\psi fN^*)}{fN^*(cN^*aem-\gamma e\kappa(1-\rho)-\alpha a\kappa\rho)}$. The eigenvalues of the characteristic polynomial (4.21) will be negative if it fulfill the Routh-Hurwitz conditions $A_i > 0$, for

$i = 1, 2, 3, 4, 5, 6$. That is, $A_1 > 0$ since it is the sum of all positives number,

$A_2 = c_2 + mc_1 + c_1c_3 + mc_3 > 0$ because it is also the sum of all positives number,

$A_3 = mc_2 + c_3c_2 + mc_3c_1 + c_4c_1 + mc_4 + \frac{\beta uf(q\kappa(1-\rho)+\kappa\rho)}{R_0 g} > 0$,

$A_4 = mc_3c_2 + c_4c_2 + mc_4c_1 + c_4c_1 + \frac{uf(\beta qf\kappa(1-\rho)+\beta\kappa\rho f)}{R_0 g} + \frac{\beta mfu(q\kappa(1-\rho)+\kappa\rho)}{R_0 g} - \theta\gamma\kappa(1-\rho)u - \theta\alpha\kappa\rho u > 0$,

$A_5 = mc_2c_4 + \frac{\beta mf^2u(q\kappa(1-\rho)+\kappa\rho)}{R_0 g} + acemfu - \theta\gamma\kappa fu(1-\rho) - \theta\kappa\rho fu\alpha - \theta\gamma\kappa(1-\rho)cu - \theta\kappa\rho a\alpha u > 0$,

$A_6 = acemfu - \theta\gamma\kappa(1-\rho)efu - \theta\kappa\rho fa\alpha u > 0$, if $u > 0$ and $acem > \theta\gamma\kappa(1-\rho) + \theta\alpha\kappa\rho a$, but $acem > \theta\gamma\kappa(1-\rho) + \theta\alpha\kappa\rho a$, let us check for $u = \beta\frac{(I+qA)}{N^*} = \frac{gcR_0}{fN^*}E^* = \frac{gcaembR_0}{fN^*(caem-\theta\gamma\epsilon\kappa(1-\rho)-\alpha\theta a\kappa\rho))}(1-\frac{1}{R_0}) \implies u > 0$ if $R_0 > 1$,

And $A_1A_2 - A_3 > 0, A_1A_2A_3 - A_3^2 - A_1^2A_4 > 0$,

$A_1A_2A_3A_4 + A_4A_5 + A_1A_2A_6 + A_2A_3A_5 + A_1A_4A_5 - A_1A_2A_5 - A_1A_4^2 - A_3^2A_4 - A_3A_6 - A_5^2 > 0$

Hence, the EEP of the model (4.1) will be locally asymptotically stable if $R_0 > 1$. □

4.4.2 Global Stability of Endemic Equilibrium Point (EEP)

Theorem 9. *The endemic equilibrium point (EEP) at E_1 of model equation (4.1) is globally asymptotically stable if $R_0 > 1$.*

Proof. To analyze the global stability of the endemic equilibrium point, we construct the Lyapunov function defined by;

$$L(S^*, V^*, E^*, A^*, I^*, R^*) = (S(t) + S^* - S^*\ln(\frac{S(t)}{S^*})) + (V(t) + V^* - V^*\ln(\frac{V(t)}{V^*})) + (E(t) + E^* - E^*\ln(\frac{E(t)}{E^*})) + (A(t) + A^* - A^*\ln(\frac{A(t)}{A^*})) + (I(t) + I^* - I^*\ln(\frac{I(t)}{I^*})) + (R(t) + R^* - R^*\ln(\frac{R(t)}{R^*})) \tag{4.22}$$

After differentiating L with respect to time it gives;

$$\begin{aligned}
\frac{dL}{dt} &= (1-\frac{S^*}{S})\frac{dS}{dt} + (1-\frac{V^*}{V})\frac{dV}{dt} + (1-\frac{E^*}{E})\frac{dE}{dt} + (1-\frac{A^*}{A})\frac{dA}{dt} + (1-\frac{I^*}{I})\frac{dI}{dt} + (1-\frac{R^*}{R})\frac{dR}{dt} \\
&= (1-\frac{S^*}{S})(\Lambda + \theta R(t) + \phi V(t) - \lambda S(t) - \psi S(t) - \mu S(t)) + (1-\frac{V^*}{V})(\psi S(t) - \phi V(t) - \mu V(t)) \\
&+ (1-\frac{E^*}{E})(\lambda S(t) - (\kappa+\mu)E(t)) + (1-\frac{A^*}{A})(\kappa(1-\rho)E(t) - (\gamma+\mu)A(t)) \\
&+ (1-\frac{I^*}{I})(\kappa\rho E(t) - (\alpha+\delta\mu)I(t))) + (1-\frac{R^*}{R})(\gamma A(t) + \alpha I(t) - (\theta+\mu)R(t)) \\
&= [\Lambda + (\lambda+\psi+\mu)S^* + (\phi+\mu)V^* + (\kappa+\mu)E^* + (\gamma+\mu)A^* + (\mu+\delta+\alpha)I^* + (\theta+\mu)R^*] \\
&- [(\Lambda + \theta R + \phi V)\frac{S^*}{S} + \psi S(t)\frac{V^*}{V} + \lambda S(t)\frac{E^*}{E} + \kappa(1-\rho)E(t)\frac{A^*}{A} + \kappa\rho E(t)\frac{I^*}{I} + (\gamma A + \alpha I)\frac{R^*}{R} \\
&+ \delta I + \mu N]
\end{aligned}$$

Let $A = [\Lambda + nS^* + fV^* + cE^* + aA^* + eI^* + mR^*]$ and $B = [(\Lambda + \theta R + \phi V)\frac{S^*}{S} + \psi S(t)\frac{V^*}{V} + \lambda S(t)\frac{E^*}{E} + \kappa(1-\rho)E(t)\frac{A^*}{A} + \kappa\rho E(t)\frac{I^*}{I} + (\gamma A + \alpha I)\frac{R^*}{R} + \delta I + \mu N]$. Then we have, $\frac{dL}{dt} = A - B$. By using this concept $\frac{dL}{dt} < 0$, if $A < B$ and $\frac{dL}{dt} = 0$ if and only if $(S^* = S, V^* = V, E^* = E, A^* = A, I^* = I, R^* = R)$. Therefore, the largest compact invariant set in $\left\{(S,V,E,A,I,R) \in \Omega;\ \frac{dL}{dt} = 0\right\}$ is a singleton E^1 which is the endemic equilibrium point of the system (4.1). Thus, by LaSalle's invariant principle (La Salle, 1976), E^1 is globally asymptotically stable. Then we have, stable in Ω if $A < B$ and $R_0 > 1$. □

4.5 Bifurcation Analysis

We used Theorem introduced in (Castillo-Chavez & Song, 2004) to determine the direction of bifurcation. In this theorem, there are two important quantities: the coefficients, say **a** and **b**, of the normal form representing the dynamics of the system on the central manifold. These coefficients decide the bifurcation. Let f_k be the k^{th} component of f and

$$\mathbf{a} = \sum_{k,i,j=1}^{6} v_k w_i w_j \frac{\partial^2 f_k}{\partial x_i \partial x_j}(0,0),\ \mathbf{b} = \sum_{k,i=1}^{6} v_k w_i \frac{\partial^2 f_k}{\partial x_i \partial \beta}(0,0) \tag{4.23}$$

In particular, if $\mathbf{a} < 0$ and $\mathbf{b} > 0$, then the bifurcation is forward. If $\mathbf{a} > 0$ and $\mathbf{b} > 0$, then the bifurcation is backward. Using this approach, we can identify the possibility of bifurcation occur for our system (4.1) at $R_0 = 1$ using Center Manifold theorem (Carr, 2012). Let $S = x_1, V = x_2, E = x_3, A = x_4, I = x_5, R = x_6$ and $N = x_1 + x_2 + x_3 + x_4 + x_5 + x_6$. Moreover, by using vector notation $x = (x_1, x_2, x_3, x_4, x_5, x_6)^T$, the system can be written in the form

$\frac{dx}{dt} = (f_1, f_2, f_3, f_4, f_5, f_6)^T$ as follow . Then model in (4.1) re-written in the form:

$$\begin{aligned}
\frac{dx_1}{dt} &= \Lambda + \theta x_6 + \phi x_2 - \lambda x_1 - \psi x_1 - \mu x_1 = f_1,\\
\frac{dx_2}{dt} &= \psi x_1 - \phi x_2 - \mu x_2 = f_2,\\
\frac{x_3}{dt} &= \lambda x_1 - (\kappa + \mu) x_3 = f_3,\\
\frac{dx_4}{dt} &= \kappa(1-\rho) x_3 - (\gamma + \mu) x_4 = f_4,\\
\frac{dx_5}{dt} &= \kappa\rho x_3 - (\alpha + \mu + \delta) x_5 = f_5,\\
\frac{dx_6}{dt} &= \gamma x_4 + \alpha x_5 - (\theta + \mu) x_6 = f_6.
\end{aligned} \tag{4.24}$$

We consider the transmission rate β as a bifurcation parameters so that $R_0 = 1$ if and only if $\beta = \beta^* = \frac{(\gamma+\mu)(\kappa+\mu)(\mu+\alpha+\delta)(\phi+\psi+\mu)}{\kappa q(1-\rho)(\alpha+\mu+\delta)(\phi+\mu)+\kappa\rho(\gamma+\mu)(\phi+\mu)}$

The disease free equilibrium is given by $\left(\frac{\Lambda(\phi+\mu)}{\mu(\psi+\phi+\mu)}, \frac{\Lambda\psi}{\mu(\psi+\phi+\mu)}, 0, 0, 0, 0\right)$. Then the linearizion matrix of (4.23) at a disease free Equilibrium is given by:

$$J(E_0) = \begin{pmatrix}
n & \phi & 0 & \frac{-\beta^* q f}{g} & \frac{-\beta^* f}{g} & \theta \\
\psi & -f & 0 & 0 & 0 & 0 \\
0 & 0 & -c & \frac{\beta^* q f}{g} & \frac{\beta^* f}{g} & 0 \\
0 & 0 & \kappa(1-\rho) & -a & 0 & 0 \\
0 & 0 & \kappa\rho & 0 & -e & 0 \\
0 & 0 & 0 & \gamma & \alpha & -m
\end{pmatrix} \tag{4.25}$$

where, $a = \gamma + \mu,\ c = \kappa + \mu,\ n = \psi + \mu,\ m = \theta + \mu,\ e = \mu + \alpha + \delta,\ g = \psi + \phi + \mu$

It is clear that 0 is a simple eigenvalue of J calculated at β^*. The right eigenvector $w = (w_1, w_2, w_3, w_4, w_5, w_6)^T$, associated with this simple zero eigenvalue can be obtained from $J.w = 0$.

$$\begin{aligned}
& n w_1 + \phi w_2 - \frac{\beta^* q f}{g} w_4 - \frac{\beta^* f}{g} w_5 + \theta w_6,\\
& \psi w_1 - f w_2 = 0,\\
& \frac{\beta^* f}{g} w_5 - c w_3 + \frac{\beta^* q f}{g} w_4 = 0,\\
& \kappa(1-\rho) w_3 - \alpha w_4 = 0,\\
& \kappa\rho w_3 - e w_5 = 0,\\
& \gamma w_4 + \alpha w_5 - m w_6 = 0.
\end{aligned} \tag{4.26}$$

From equation (4.26) we consider

$w_1 = \left(\frac{\beta^* q f \kappa(1-\rho)e}{\alpha g(n+\phi\psi)} + \frac{\beta^* f \kappa \rho}{ge(n+\phi\psi)} - \frac{\theta\kappa(\gamma(1-\rho)e+\alpha^*\rho)}{em(n+\phi\psi)}\right) w_3, \quad w_2 = \frac{\psi w_1}{f}, \quad w_2 > 0, \quad w_3 > 0,$

$w_4 = \frac{\kappa(1-\rho)w_3}{\alpha}\ w_5 = \frac{\kappa\rho w_3}{e}, \quad w_6 = \frac{(\kappa\gamma(1-\rho)e+\alpha^2\kappa\rho)W_3}{em}.$

Next we compute the left eigenvector $v.J = 0, \quad v = (v_1, v_2, v_3, v_4, v_5, v_6)^T$.

$v_1 = v_2 = v_6 = 0, v_3 > 0, v_4 = \frac{\beta^* q f}{ga} v_3, v_5 = \frac{\beta^* f}{ge} v_3$

Computation of a: To evaluate **a**, we use the following partial derivatives. Since the first, the second and sixth component of v are zero, we don't need the derivatives of f_1, f_2 and f_6. From the derivatives of f_3, f_4 and f_5 the only ones that are nonzero are the following:

$\frac{\partial^2 f_3}{\partial x_4 \partial x_1} = \frac{\partial^2 f_3}{\partial x_1 \partial x_4} = \frac{\mu\beta^* q}{\Lambda}, \frac{\partial^2 f_3}{\partial x_5 \partial x_1} = \frac{\partial^2 f_3}{\partial x_1 \partial x_5} = \frac{\mu\beta^*}{\Lambda}$

then we get

$$\begin{aligned}\mathbf{a} &= 2v_3[w_1 w_4 \frac{\mu\beta^* q}{\Lambda} + w_1 w_5 \frac{\mu\beta^*}{\Lambda}] = 2v_3 \frac{\mu\beta^*}{\Lambda} w_1[w_4 q + w_5] \\ &= 2\frac{\mu\beta^*}{\Lambda} v_3[\frac{\beta^* q f \kappa(1-\rho)e}{\alpha g(n+\phi\psi)} + \frac{\beta^* f \kappa\rho}{ge(n+\psi\phi)} - \frac{\theta\kappa(\gamma(1-\rho)e+\alpha^*\rho)}{em(n+\psi\phi)}][\frac{\kappa(1-\rho)}{\alpha} q + \frac{\kappa\rho}{e}] w_3^2\end{aligned}$$

Computation of b: We find the following partial derivatives to evaluate **b**.

$\frac{\partial^2 f_3}{\partial x_4 \partial \beta} = \frac{q(\psi+\mu)}{\phi+\psi+\mu}, \frac{\partial^2 f_3}{\partial x_5 \partial \beta} = \frac{\psi+\mu}{\phi+\psi+\mu}$, then we obtain $b = q v_3 w_4 + v_3 w_5 > 0$

Since all the terms in the expressions of **b** are positive ($\mathbf{b} > 0$), the presence of the bifurcation at $\beta = \beta^*$ depends only on the sign of **a**. Forward bifurcation occurs if and only if $\frac{\beta^* q f \kappa(1-\rho)e}{\alpha g(n+\psi\phi)} + \frac{\beta^* f \kappa\rho}{ge(n+\psi\phi)} > \frac{\theta\kappa(\gamma(1-\rho)e+\alpha^*\rho)}{em(n+\psi\phi)}$.

4.6 Sensitivity Analysis

Sensitivity analysis of the basic reproductive number can be used to design a mitigation strategy to slow the spread of the pandemic by reducing R_0. Sensitivity analysis (Sanchez & Blower, 1997) for the basic reproductive number mainly helps to discover parameters that have a high impact on the values of R_0 and hence should be targeted for designing intervention strategy. The following definition is used to find the sensitivity index of each of the parameters involved in R_0.

Definition 4.6.1. *Normalized forward sensitivity index of R_0 which is differentiable with respect to a given parameter P is defined as (Chitnis et al., 2008)*

$$\Phi_p^{R_0} = \frac{p}{R_0} \frac{\partial R_0}{\partial p} \tag{4.27}$$

The explicit expression of R_0 is given by
$R_0 = \frac{\beta q(\alpha+\mu+\delta)\kappa(1-\rho)(\phi+\mu)+\beta\kappa\rho(\gamma+\mu)(\phi+\mu)}{(\gamma+\mu)(\kappa+\mu)(\mu+\alpha+\delta)(\psi+\phi+\mu)}$.

$$\Phi_{\beta}^{R_0} = \frac{\beta}{R_0}\frac{\partial R_0}{\partial \beta} = 1 > 0,\ \Phi_{\kappa}^{R_0} = \frac{\kappa}{R_0}\frac{\partial R_0}{\partial \kappa} = \frac{\mu}{\kappa+\mu} > 0,$$
$$\Phi_{q}^{R_0} = \frac{q}{R_0}\frac{\partial R_0}{\partial q} = \frac{q(1-\rho)(\alpha+\mu+\delta)}{q(1-\rho)(\alpha+\mu+\delta)+\rho(\gamma+\mu)} > 0,$$
$$\Phi_{\rho}^{R_0} = \frac{\rho}{R_0}\frac{\partial R_0}{\partial \rho} = \frac{\rho(\gamma+\mu)-\rho q(\alpha+\mu+\delta)}{q(1-\rho)(\alpha+\mu+\delta)+\rho(\gamma+\mu)},$$
$$\Phi_{\alpha}^{R_0} = \frac{-\alpha\rho(\gamma+\mu)}{(q(1-\rho)(\alpha+\mu+\delta)+\rho(\gamma+\mu))(\alpha+\mu+\delta)} < 0,$$
$$\Phi_{\delta}^{R_0} = \frac{-\delta\rho(\gamma+\mu)}{q(1-\rho)(\alpha+\mu+\delta)+\rho(\gamma+\mu)(\alpha+\mu+\delta)} < 0,\ \Phi_{\psi}^{R_0} = \frac{-\psi}{\phi+\psi+\mu} < 0,$$
$$\Phi_{\phi}^{R_0} = \frac{\phi\psi}{(\phi+\mu)(\psi+\phi+\mu)} > 0,\ \Phi_{\gamma}^{R_0} = \frac{-\gamma q(1-\rho)(\alpha+\mu+\delta)}{(q(1-\rho)(\alpha+\mu+\delta)+\rho(\gamma+\mu))(\gamma+\mu)} < 0,$$
$$\Phi_{\mu}^{R_0} = \mu(\frac{1}{\phi+\mu} + \frac{q(1-\rho)+\rho}{q(1-\rho)(\alpha+\mu+\delta)+\rho(\gamma+\mu)} - (\frac{1}{\gamma+\mu} + \frac{1}{\kappa+\mu} + \frac{1}{\mu+\alpha+\delta} + \frac{1}{\psi+\phi+\mu})).$$

The sensitivity indices of the basic reproductive number with respect to the main parameters are arranged in Table 4.3. Those parameters that have positive indices, β, k, ϕ, and q show that they have great impact on expanding the disease in the population if their values are increasing. The basic reproduction number increases as their values increase, it means that the average number of secondary cases of infection increases in the population.

Table 4.3: Sensitivity Indices of the Basic Model Parameters in R_0

Parameter	Description	Sensitivity indices
β	Effective contact rate of infection	+ 1
κ	Per capita rate of becoming infectious	+ 0.0003955942
q	Transmission rate for asymptomatic individuals	+ 0.0240509051
ρ	Probability of exposed individuals joining infectious class	+ 0.1998944899
α	Progression from compartment $I(t)$ to $R(t)$ due to effective treatment	- 0.9752592058
δ	Death rate due to disease in the symptomatic compartment	- 0.0003996834
ϕ	The rate vaccine wanes	+ 0.1736810451
ψ	The transmission rate of susceptible into vaccinated class	- 0.1737013346
γ	Rate at which asymptomatic individuals recovered	- 0.0246472422
μ	Natural death rate	- 0.0073343

Furthermore, those parameters in which their sensitivity indices are negative δ, ψ, γ and α have an influence of minimizing the burden of the disease in the community as their values

increase. And also as their values increase, the basic reproduction number decreases, which leads to minimizing the endemic nature of the disease in the community. Parameter values are taken from Table 4.2.

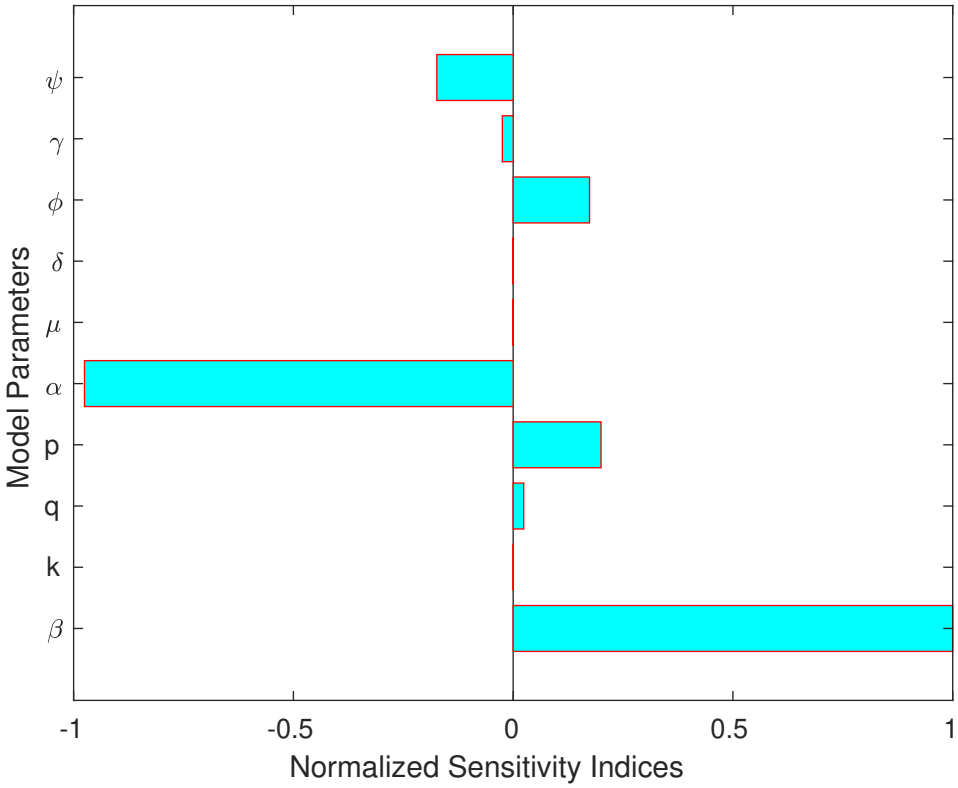

Figure 4.2: Figure Normalized sensitivity indices of R_0 with respect to parameters of the model (4.1).

CHAPTER 5

MATHEMATICAL MODEL FOR COVID-19 WITH TIME DELAY

This chapter presents a deterministic mathematical model for COVID-19 pandemic using a system of nonlinear delay differential equations. Model description and analysis are also detailed in order.

5.1 Model Description and Formulation

In this section, we consider Delayed SVEAIR type mathematical modeling for the dynamics of COVID-19 pandemic. The total population $N(t)$ is divided into six compartments: Susceptible $S(t)$, Vaccinated $V(t)$, Exposed $E(t)$, Asymptomatic A(t), Infected $I(t)$ and Recovered $R(t)$ population at time $t \geq 0$. Thus, total population is given by

$$N(t) = S(t) + V(t) + E(t) + A(t) + I(t) + R(t)$$

The description of all the state variables and parameters are given in Table 4.1 and Table 4.2 respectively. The disease is assumed to have incubation period of the virus τ. The incubation represents the delay time from exposure to the development of symptoms of the virus. The transmission incidence will be a function of $(t - \tau)$. The compartmental epidemic system for

COVID-19 is governed by the system of nonlinear delay differential equations:

$$\begin{aligned}
\frac{dS(t)}{dt} &= \Lambda + \theta R(t) + \phi V(t) - \lambda S(t) - \psi S(t) - \mu S(t),\\
\frac{dV(t)}{dt} &= \psi S(t) - \phi V(t) - \mu V(t),\\
\frac{dE(t)}{dt} &= \lambda S(t) - \kappa E(t-\tau) - \mu E(t),\\
\frac{dA(t)}{dt} &= \kappa(1-\rho)E(t-\tau) - (\gamma+\mu)A(t),\\
\frac{dI(t)}{dt} &= \kappa\rho E(t-\tau) - (\mu+\delta+\alpha)I(t),\\
\frac{dR(t)}{dt} &= \gamma A(t) + \alpha I(t) - (\theta+\mu)R(t).
\end{aligned} \tag{5.1}$$

The initial conditions are given as $S(\sigma) = \Psi_1(\sigma) > 0, V(\sigma) = \Psi_2(\sigma) \geq 0, E(\sigma) = \Psi_3(\sigma) \geq 0, A(\sigma) = \Psi_4(\sigma) \geq 0, I(\sigma) = \Psi_5(\sigma) \geq 0, R(\sigma) = \Psi_6(\sigma) \geq 0,\ \sigma \in [-\tau, 0]$. Where $\Psi = (\Psi_1, \Psi_2, \Psi_3, \Psi_4, \Psi_5, \Psi_6)^T \in C$, C is Banach space of continuous functions $C([-\tau, 0], \mathbb{R}^6)$ mapping the interval $[-\tau, 0]$ into $\mathbb{R}^6_+$ where $\Psi_i,\ i = 1, 2, 3, 4, 5, 6$ are non-negative continuous initial functions on $[-\tau, 0]$.

5.2 Model Analysis

5.2.1 Invariant Region

Let us determine a region in which the solution of model (5.1) is bounded. For this model the total population in time t is given by $N(t) = S(t) + V(t) + E(t) + A(t) + I(t) + R(t)$ Then, differentiating N with respect to time we obtain:
$\frac{dN(t)}{dt} = \frac{S(t)}{dt} + \frac{dV(t)}{dt} + \frac{dE(t)}{dt} + \frac{dA}{dt} + \frac{I(t)}{dt} + \frac{dR(t)}{dt} = \Lambda - \delta I(t) - \mu N(t).$
If there is no death due to the disease, we get

$$\begin{aligned}
\frac{dN(t)}{dt} &\leq \Lambda - \mu N\\
N'(t) + \mu N(t) &\leq \Lambda.
\end{aligned} \tag{5.2}$$

By integrating factor,

$$\frac{d(N(t)e^{\mu t})}{dt} \leq \Lambda e^{\mu t}. \tag{5.3}$$

Integrating both sides of the equation 5.3 and simplifying it, then we have

$$N(t) \leq \frac{\Lambda}{\mu} + ce^{-\mu t}. \tag{5.4}$$

As $t \longrightarrow \infty$ in equation 5.4, the population size $N(t) \longrightarrow \frac{\Lambda}{\mu}$, which implies that $0 < N(t) \leq \frac{\Lambda}{\mu}$. Thus the feasible region of the system 5.1is given by the set

$$\Omega = \left\{(S, V, E, A, I, R) \in \mathbb{R}^6_+ : 0 \leq N(t) < \frac{\Lambda}{\mu}\right\} \tag{5.5}$$

is positively invariant. That is; $\frac{dS}{dt}|_{S=0} = \Lambda + \theta R + \phi V > 0$, $\frac{dV}{dt}|_{v=0} = \phi S \geq 0$, $\frac{dE}{dt}|_{E=0} = \lambda S \geq 0$, $\frac{dA}{dt}|_{A=0} = \kappa(1-\rho)E(t-\tau) \geq 0$, $\frac{dI}{dt}|_{I=0} = \kappa\rho E(t-\tau) \geq 0$, $\frac{dR}{dt}|_{R=0} = \gamma A + \alpha I(t) \geq 0$. Consequently, this region attracts all solutions of the system and this restricted region will be enough to consider of the dynamics of the model (5.1).

5.2.2 Existence and Uniqueness of the Solution

The validity and authenticity of any mathematical model depends on the existence and uniqueness of the solutions for the governing system of equations.

Theorem 10. *Let $t_0 > 0$ and the initial conditions satisfies $S(\sigma) > 0$, $V(\sigma) \geq 0$, $E(\sigma) \geq 0$, $A(\sigma) \geq 0$, $I(\sigma) \geq 0$, $R(\sigma) \geq 0$ in the prescribed region Ω. Then the solution of the model system (5.1) exists and unique in $\mathbb{R}^6_+$.*

Proof. The right hand side of the model equation 5.1 can be expressed as follows:

$$\begin{aligned}
f_1(S, V, E, A, I, R) &= \Lambda + \theta R(t) + \phi V(t) - \lambda S(t) - (\psi + \mu)S(t),\\
f_2(S, V, E, A, I, R) &= \psi S(t) - (\phi + \mu)V(t),\\
f_3(S, V, E, A, I, R) &= \lambda S(t) - \kappa E(t-\tau) - \mu E(t),\\
f_4(S, V, E, A, I, R) &= \kappa(1-\rho)E(t-\tau) - (\gamma + \mu)A(t),\\
f_5(S, V, E, A, I, R) &= \kappa\rho E(t-\tau) - (\alpha + \delta + \mu)I(t),\\
f_6(S, V, E, A, I, R) &= \gamma A(t) + \alpha I(t) - (\theta + \mu)R(t).
\end{aligned}$$

Let Ω denote the region $\Omega = \left\{(S, V, E, A, I, R) \in \mathbb{R}^6_+ : N(t) \leq \frac{\Lambda}{\mu}\right\}$. Then equations 5.1 have a unique solution if $\frac{\partial f_i}{\partial x_j}$, $i, j = 1, 2, ..., 6$, are continuous and bounded in Ω. Here, using notations $x_1 = S$, $x_2 = V$, $x_3 = E$, $x_4 = A$, $x_5 = I$, $x_6 = R$. When we differentiate the

system $\frac{\partial f_i}{\partial x_j}$ it is continuous and bounded in Ω (Hale & Lunel, 2013). Here, observe that f has a continuous first partial derivative with respect to each state variables in $\mathbb{R}^6_+$. It follows that f is locally Lipschitz. Thus, the result is the direct outcome of fundamental existence and uniqueness theorem in $\mathbb{R}^6_+$. □

5.2.3 Non-negativity of Solutions

Theorem 11. *If* $S(\sigma) > 0,\ V(\sigma) \geq 0,\ E(\sigma) \geq 0,\ A(\sigma) \geq 0,\ I(\sigma) \geq 0,\ R(\sigma) \geq 0$ *are all non-negative, then the solutions* $S(t),\ V(t),\ E(t),\ A(t),\ I(t),$ *and* $R(t)$ *are all positive for* $t > 0$ *by arranging parameters and initial conditions.*

Proof. From the system of differential equation 5.1, let us take the first equation:

$$\frac{dS(t)}{dt} = \Lambda + \theta R(t) + \phi V(t) - \lambda S(t) - \psi S(t) - \mu S(t),$$

This equation can be expressed without loss of generality, after eliminating the positive term

$$(\Lambda + \theta R + \phi V),$$

as an inequality

$$\frac{dS}{dt} > -(\frac{\beta(I + qA)}{N} + \psi + \mu)S,$$

Then using separable method of variables and applying integration, the solution of the deferentially inequality can be obtained as

$$S(t) > \Psi_1(0)e^{-\psi t - \mu t - \int_0^t \frac{\beta(I+qA)}{N} dt} \geq 0.$$

Where $S(\sigma)$ is obtain from initial condition. Since exponential function is always non-negative, the function $e^{-\psi t - \mu t - \int_0^t \frac{\beta(I+qA)}{N} dt}$ is non-negative quantity. Hence, we conclude that $S(t) > 0$.

Similarly, the second equation for the system 5.1 is given by

$$\frac{dV(t)}{dt} = \psi S(t) - (\phi + \mu)V(t),$$

after eliminating the positive term $\psi S(t)$ as an inequality as

$$\frac{dV(t)}{dt} \geq -(\phi + \mu)V,$$

Using separable method of variables and on applying integration, the solution of the foregoing differentially inequality can be obtained as

$$V(t) \geq \Psi_2(0)e^{-(\phi+\mu)t},$$

Where Ψ_2 is obtain from initial condition. Recall that an exponential function is always non-negative irrespective of the sign of the exponent, i.e, the exponential function $e^{-(\phi+\mu)t}$ is non-negative quantity. Hence, we can conclude that $V(t) \geq 0$.
Similarly by Hale & Lunel (2013), we obtain

$$E(t) \geq \Psi_3(0)e^{-\mu t} - \kappa \int_0^t e^{(s-t)\mu} E(s-\tau)ds > 0,$$

This indicate that $E(t)$ is negative if $\kappa \int_0^t e^{(s-t)\mu} E(s-\tau)ds$ is greater than the positive part of the equation. But we have a Banach space of continuous initial functions this implies that we have also Banach space continuous function by using invariant region. Thus we have positive function on describe region even if $E(t) < 0$.

$$A(t) \geq \Psi_4(0)e^{-(\gamma+\mu)t} > 0,$$
$$I(t) \geq \Psi_5(0)e^{-(\alpha+\mu+\delta)t} > 0,$$
$$R(t) \geq \Psi_6(0)e^{-(\theta+\mu)t} > 0.$$

This proves that the solution of system (5.1) are positive for all $t \geq 0$. □

5.2.4 COVID Free Equilibrium Point

Solving for the non-infected state variable by using delay has no effect on equilibrium point; that means at $\tau = 0$. We obtain the disease free equilibrium point
$E_0 = \left(\frac{\Lambda(\phi+\mu)}{\mu(\psi+\phi+\mu)}, \frac{\psi\Lambda}{\mu(\psi+\phi+\mu)}, 0, 0, 0, 0\right)$.

5.2.5 The Basic Reproduction Number

In this section, we determine the basic reproduction number. The delay doesn't impact on reproduction number. Therefore,

$R_0 = \frac{\beta q f \kappa e(1-\rho)+\beta\kappa\rho a f}{gaec} = \frac{\beta q(\alpha+\mu+\delta)\kappa(1-\rho)(\phi+\mu)+\beta\kappa\rho(\gamma+\mu)(\phi+\mu)}{(\gamma+\mu)(\kappa+\mu)(\mu+\alpha+\delta)(\phi+\psi+\mu)}$.

5.2.6 Endemic Equilibrium Point

The Endemic equilibrium point which denoted by E_1 is a steady state solution where the disease persists in the population. The endemic equilibrium $E_1 = (S^*, V^*, E^*, A^*, I^*, R^*)$ in this section is the same with the non-delay part.

5.3 Stability Analysis of Covid-19 Free Equilibrium Point

5.3.1 Local Stability of Covid-19 Free Equilibrium Point

Theorem 12. *The disease-free equilibrium* $E_0 = \left(\frac{\Lambda(\phi+\mu)}{\mu(\phi+\psi+\mu)}, \frac{\psi\Lambda}{\mu(\phi+\psi+\mu)}, 0, 0, 0, 0\right)$ *of the system (5.1) is locally asymptotically stable if* $R_0 < 1$.

Proof. The Jacobian matrix at the disease-free equilibrium E_0 of the system (5.1) is

$$J(E_0) = \begin{bmatrix} -n & \phi & 0 & \frac{-\beta q f}{g} & \frac{-\beta f}{g} & \theta \\ \psi & -f & 0 & 0 & 0 & 0 \\ 0 & 0 & -\mu-\kappa e^{-\lambda\tau} & \frac{\beta q f}{g} & \frac{\beta f}{g} & 0 \\ 0 & 0 & \kappa(1-\rho)e^{-\lambda\tau} & -a & 0 & 0 \\ 0 & 0 & \kappa\rho e^{-\lambda\tau} & 0 & -e & 0 \\ 0 & 0 & 0 & \gamma & \alpha & -m \end{bmatrix} \tag{5.6}$$

where; $e = \alpha+\mu+\delta, a = \gamma+\mu, n = \psi+\mu, m = \theta+\mu, f = \phi+\mu, g = \phi+\psi+\mu$. The eigenvalues of $J(E_0)$ are the solutions of the characteristics equation $det\,[J(E_0) - \lambda I_6] = 0$,

where I_6 is an identity matrix of order 6. Then we have

$$|J(E_0) - \lambda I_6| = \begin{vmatrix} -n-\lambda & \phi & 0 & \frac{-\beta q f}{g} & \frac{-\beta f}{g} & \theta \\ \psi & -f-\lambda & 0 & 0 & 0 & 0 \\ 0 & 0 & -\mu-\kappa e^{-\lambda\tau}-\lambda & \frac{\beta q f}{g} & \frac{\beta f}{g} & 0 \\ 0 & 0 & \kappa(1-p)e^{-\lambda\tau} & -a-\lambda & 0 & 0 \\ 0 & 0 & \kappa\rho e^{-\lambda\tau} & 0 & -e-\lambda & 0 \\ 0 & 0 & 0 & \gamma & \alpha & -m-\lambda \end{vmatrix} = 0$$

The corresponding characteristic equation has the following form:

$$(-n-\lambda)(-f-\lambda)[(-\mu-\kappa e^{-\lambda\tau}-\lambda)(-a-\lambda)(-e-\lambda)(-m-\lambda) + \frac{\beta f\kappa\rho e^{-\lambda\tau}(a+\lambda)(-m-\lambda)}{g} + \frac{\beta q f\kappa(1-\rho)e^{-\lambda\tau}(e+\lambda)(-m-\lambda)}{g}] - \psi\phi[(-\mu-\kappa e^{-\lambda\tau}-\lambda)(-a-\lambda)(-e-\lambda)(-m-\lambda) + \frac{\beta\kappa\rho f e^{-\lambda\tau}(a+\lambda)(-m-\lambda)}{g} + \frac{\beta q f\kappa(1-\rho)e^{-\lambda\tau}(e+\lambda)(-m-\lambda)}{g}] = 0 \tag{5.7}$$

Then solving equation (5.7) we obtain,

$$-m-\lambda = 0, (-n-\lambda)(-f-\lambda) - \psi\phi = 0, (-\mu-\kappa e^{-\lambda\tau}-\lambda)(-a-\lambda)(-e-\lambda) + \frac{\beta f\kappa q(1-\rho)e^{-\lambda\tau}(e+\lambda)}{g} + \frac{\beta f\kappa\rho e^{-\lambda\tau}(a+\lambda)}{g} = 0. \tag{5.8}$$

Clearly, the sign of the first eigenvalue $\lambda_1 = -m$ is negative. To determine the value of the left eigenvalues

$$(-n-\lambda)(-f-\lambda) - \psi\phi = \lambda^2 + (n+f)\lambda + nf - \psi\phi = 0,$$
$$\lambda_2 = \frac{-n-f-\sqrt{(n+f)^2-4\mu g}}{2}, \lambda_3 = \frac{-n-f+\sqrt{(n+f)^2-4\mu g}}{2}.$$

The eigenvalue of λ_2 and λ_3 are negative because of $\mu g > 0$. The sign of the remaining eigenvalues which state that the roots of the characteristic equation:

$$\lambda^3 + a_1\lambda^2 + a_2\lambda + a_3 + (b_1\lambda^2 + b_2\lambda + b_3)e^{-\lambda\tau} = 0. \tag{5.9}$$

where, $a_1 = e + a + \mu$, $a_2 = ae + a\mu + e\mu$, $a_3 = ae\mu$, $b_1 = \kappa$, $b_2 = \kappa(a + e - \frac{\beta f(q(1-\rho)+\rho)}{g})$,

$b_3 = \kappa ae - R_0 ace$ is real distinct and negative eigenvalues if $\tau = 0$ as we discussed on Theorem 6. Now this equation is not suitable for Routh-Hurwitz criteria and also the solution doesn't exist on real if $\tau > 0$. Notice 0 is not a root of (5.9) because $R_0 < 1$. We define $\lambda = iw$ $(w > 0)$ is a purely imaginary root of (5.9). Then we get

$$\begin{aligned} w^3 - a_2 w &= (b_1 w^2 - b_3) sin(w\tau) + b_2 w cos(w\tau) \\ a_3 - a_1 w^2 &= (b_1 w^2 - b_3) cos(w\tau) - b_2 w sin(w\tau) \end{aligned} \tag{5.10}$$

Squaring and adding both equations of (5.10), it follows that

$$H(w) = w^6 + (a_1^2 - b_1^2 - 2a_2)w^4 + (a_2^2 + 2b_1 b_3 - 2a_1 a_3 - b_2^2)w^2 + a_3^2 - b_3^2 \tag{5.11}$$

Let $z = w^2, c_1 = a_1^2 - b_1^2 - 2a_2, c_2 = a_2^2 + 2b_1 b_3 - 2a_1 a_3 - b_2^2, c_3 = a_3^2 - b_3^2$ then equation (5.11) becomes

$$H(z) = z^3 + c_1 z^2 + c_2 z + c_3$$

This indicate that if $R_0 < 1$, $c_1 > 0$, $c_3 > 0$, $c_2 > 0$, z has negative eigenvalue that means there is no positive real w where λ is complex. Therefore the DFE is locally asymptotically stable if $R_0 < 1$. □

5.3.2 Global Stability of the COVID Free Equilibrium Point

Theorem 13. *The disease free equilibrium of the system (4.1) is globally asymptotically stable if $R_0 < 1$ for all $\tau > 0$.*

Proof. Let $\Omega \subseteq \mathbb{R}_+$ be an open neighborhood of the disease free equilibrium point E_0. Then define the Lyapunove function L, defined by:

$$L = B_1 E + B_2 A + B_3 I + B_3 \kappa \rho \int_{t-\tau}^{t} E(s)ds - B_1 \kappa \int_{t-\tau}^{t} E(s)ds + B_2 \kappa (1-\rho) \int_{t-\tau}^{t} E(s)ds \tag{5.12}$$

Where B_i, for $i = 1, 2, 3$ are some positive constants. The Lyapunov function L is continuously differentiable as the functions of E, A, I and $L(E_0) = 0$ as well as $L > 0$,

$\forall(S,V,E,A,I,R) \in \mathbb{R}^6_+ - \{E_0\}$. Now differentiating L with respect to time we obtain

$$\begin{aligned}
\frac{dL}{dt} &= B_1(\frac{\beta(I+qA)}{N}S - cE) + B_2(\kappa(1-\rho)E - aA) + B_3(\kappa\rho E - e)I \\
&\leq B_1(\frac{\beta f(I+qA)}{g} - cE) + B_2(\kappa(1-\rho)E - aA)) + B_3(\kappa\rho E - e)I, \ since \ \frac{S}{N} \leq \frac{f}{g} \\
&= (B_2\kappa(1-\rho) - B_1(\kappa+\mu) + B_3\kappa\rho)E + (\frac{\beta B_1 qf}{g} - aB_2)A + (\frac{\beta B_1 f}{g} - B_3)I \\
&= B_1c(\frac{B_2\kappa(1-\rho) + B_3\kappa\rho}{B_1c} - 1)E + (\frac{\beta B_1 qf}{g} - aB_2)A + (\frac{\beta B_1 f}{g} - B_3e)I
\end{aligned}$$

Now choosing $B_1 = gea, B_2 = \beta qef, B_3 = \beta af$; then we have

$$\begin{aligned}
\frac{dL}{dt} &\leq geca(\frac{\beta qef\kappa(1-\rho) + \beta af\kappa\rho}{geac} - 1)E + (\beta eaqf - a\beta qef)A + (\beta eaf - \beta afe)I \\
&= geca(\frac{\beta qef\kappa(1-\rho) + \beta af\kappa\rho}{geac} - 1)E + 0.
\end{aligned}$$

This implies that $\frac{dL}{dt} \leq geca(R_0 - 1)E$. Hence, $\frac{dL}{dt} \leq 0$ For $R_0 \leq 1$ and $\frac{dL}{dt} = 0$ if and only if $E = 0$. Therefore, the largest compact invariant set in Ω is the singleton set $(\frac{\Lambda(\phi+\mu)}{\mu(\phi+\psi+\mu)}, \frac{\psi\Lambda}{\mu(\phi+\psi+\mu)}, 0, 0, 0, 0)$. Hence, by LaSalle's invariant principle (La Salle, 1976), every solution to equations of model (5.1) with initial conditions in Ω which approaches the disease-free equilibrium point as time t tends to infinity whenever $R_0 < 1$. This implies that the disease-free equilibrium is globally asymptotically stable in Ω. □

5.4 Stability Analysis of Endemic Equilibrium Point

The endemic equilibrium point denoted by $E_1 = (S^*, V^*, E^*, A^*, I^*, R^*)$ is a steady state solution where the disease persists in the population. It is determined above by setting rates of changes of variables with respect to time in the model equation (5.1) to zero.

5.4.1 Local Stability of Endemic Equilibrium Point (EEP)

Theorem 14. *The Endemic equilibrium Point (EEP) of system (5.1) at E_1 is locally asymptotically stable or may undergoes a Hopf bifurcation if $R_0 > 1$.*

Proof. To proof the local stability of endemic equilibrium point of the system (5.1) we use linearization approach. Thus, the Jacobian $J(E_1)$ matrix at the endemic equilibrium point

becomes

$$J(E_1) = \begin{bmatrix} -n & \phi & 0 & \frac{-\beta q f}{R_0 g} & \frac{-\beta f}{R_0 g} & \theta \\ \psi & -f & 0 & 0 & 0 & 0 \\ u & 0 & -\kappa e^{-\lambda\tau} - \mu & \frac{\beta q f}{R_0 g} & \frac{\beta f}{R_0 g} & 0 \\ 0 & 0 & \kappa(1-\rho)e^{-\lambda\tau} & -a & 0 & 0 \\ 0 & 0 & \kappa\rho e^{-\lambda\tau} & 0 & -e & 0 \\ 0 & 0 & 0 & \gamma & \alpha & -m \end{bmatrix} \tag{5.13}$$

where $u = \frac{\beta(qA^*+I^*)}{N^*}$, $a = \gamma + \mu$, $f = \phi + \mu$, $n = u + \psi + \mu$, $m = \theta + \mu$, $e = \mu + \alpha + \delta$, $g = \phi + \psi + \mu$. The characteristic equation of the Jacobian matrix (5.13) at the endemic equilibrium point is also given by:

$$(-m-\lambda)((-n-\lambda)(-f-\lambda) - \phi\psi)[(-\kappa e^{-\lambda\tau} - \mu - \lambda)(-a-\lambda)(-e-\lambda) + \frac{\beta q f \kappa e^{-\lambda\tau}(1-\rho)(e+\lambda)}{R_0 g}$$
$$+ \frac{\beta\kappa p f e^{-\lambda\tau}(a+\lambda)}{R_0 g}] + \frac{\beta q f u \kappa (f+\lambda)}{R_0 g}(1-\rho)e^{-\lambda\tau}(-e-\lambda)(-m-\lambda) - \frac{\beta\kappa\rho f u e^{-\lambda\tau}}{R_0 g}(f+\lambda)(a+\lambda)$$
$$(-m-\lambda) - \theta(f+\lambda)u[\kappa(1-\rho)\gamma e^{-\lambda\tau}(e+\lambda) + \kappa\rho\alpha e^{-\lambda\tau}(a+\lambda)] = 0.$$

After some arrangements the characteristic equation becomes,

$$\lambda^6 + p_1\lambda^5 + p_2\lambda^4 + p_3\lambda^3 + p_4\lambda^2 + p_5\lambda + p_6 + (q_1\lambda^5 + q_2\lambda^4 + q_3\lambda^3 + q_4\lambda^2 + q_5\lambda + q_6)e^{-\lambda\tau} = 0. \tag{5.14}$$

Where

$p_1 = a_1 + b_1,\ p_2 = b_2 + a_2 + a_1 b_1,\ p_3 = b_3 + a_1 b_2 + b_1 a_2 + a_3,\ A_4 = a_1 b_3 + a_2 b_2 + a_3 b_1,$

$p_5 = a_2 b_3 + a_3 b_2,\ \ p_6 = a_3 b_3, q_1 = c_1, q_2 = c_2 + a_1 c_1,\ \ q_3 = c_3 + a_1 c_2 + c_1 a_2 + \frac{\beta f \kappa u(q(1-\rho)+\rho)}{R_0 g},$

$q_4 = a_1 c_3 + a_2 c_2 + a_3 c_1 + aceu + \frac{\beta\kappa f u(m+f)(q(1-\rho)+\rho)}{R_0 g} - \theta u\kappa(\rho\alpha + \gamma(1-\rho)),$

$q_5 = a_2 c_3 + a_3 c_2 + aceu(m+f) + \frac{\beta\kappa m f^2 u(q(1-\rho)+\rho)}{R_0 g} - \theta\kappa u(\alpha\rho(a+f) + \gamma(1-\rho)(e+f)),$

$q_6 = a_3 c_3 + mfaceu - \theta u\kappa f[\gamma e(1-\rho) + \rho\alpha a],$

$Hence,\ \ a_1 = u + \psi + \phi + 2\mu + m,\ \ a_2 = mu + m\psi + m\phi + 2\mu m + u\phi + m\phi + u\mu + \psi\mu + \mu^2,$

$a_3 = m(u\phi + \phi\mu + u\mu + \psi\mu + \mu^2),\ \ b_1 = a + e + \mu,\ \ b_2 = a\mu + e\mu + ae,\ \ b_3 = ae\mu,\ c_1 = \kappa,$

$c_2 = \kappa(a + e - \frac{\beta\kappa f(q(1-\rho)+\rho)}{R_0 g}),\ c_3 = ae\kappa - aec.X$

Here (5.14) has real and negative root if $\tau = 0$ in Theorem 8. When $\tau > 0$, notice 0 is not a root of (5.14) because of $R_0 > 1$. We define $\lambda = iw(w > 0)$ is a purely imaginary root of (5.14). Then we get:

$$\begin{aligned} p_1 w^5 - p_3 w^3 + p_5 w &= (-q_1 w^5 + q_3 w^3 - q_5 w)cos(w\tau) + (q_2 w^4 - q_4 w^2 + q_6)sin(w\tau) \\ w^6 - p_2 w^4 + p_4 w^2 - p_6 &= (q_2 w^4 - q_4 w^2 + q_6)cos(w\tau) + (q_1 w^5 - q_3 w^3 + q_5 w)sin(w\tau) \end{aligned} \tag{5.15}$$

Squaring and adding both equations of (5.15), it follows that where $x = w^2$ and

$$d_1 = p_1^2 - 2p_2 - q_1^2,\ \ d_2 = p_2^2 + 2p_4 - 2p_1p_3 + 2q_1q_3 - q_2^2,$$
$$d_3 = p_3^2 + 2p_1p_5 - 2p_2p_4 - 2p_6 - q_3^2 - 2q_1q_5 + 2q_2q_4,\ \ d_4 = p_4^2 + 2p_2p_6 - 2p_3p_5 + 2q_3q_5$$
$$- q_4^2 - 2q_2q_6,\ \ d_5 = p_5^2 - p_4p_6 - q_5^2 + 2q_4q_6,\ \ d_6 = p_6^2 - q_6^2,$$

$$x^6 + d_1x^5 + d_2x^4 + d_3x^3 + d_4x^2 + d_5x + d_6 = 0 \tag{5.16}$$

Assume that equation (5.16) has a positive root. Eliminating sin(wτ) from equation (5.15) we obtain

$$\tau_n = \frac{1}{w_n} cos^{-1}\left(\frac{(w_n^6 - p_2w_n^4 + p_4w_n^2 - p_6)(q_2w_n^4 - q_4w_n^2 + q_6) - (p_1w_n^5 - p_3w_n^3 + p_5w_n)(q_1w_n^5 - q_3w_n^3 + q_5w_n)}{(q_1w_n^5 - q_3w_n^3 + q_5w_n)^2 + (q_2w_n^4 - q_4w_n^2 + q_6)^2}\right) + \frac{2n\pi}{w_n}, n = 0, 1, ... \tag{5.17}$$

Let τ_0 be the smallest of τ_n at which $\lambda = \pm iw_0$, $(w_0 = w(\tau_0))$ be a root of (5.14) and defined by:

$$\tau_0 = \frac{1}{w_0} cos^{-1}\left(\frac{(w_0^6 - p_2w_0^4 + p_4w_0^2 - p_6)(q_2w_0^4 - q_4w_0^2 + q_6) - (p_1w_0^5 - p_3w_0^3 + p_5w_0)(q_1w_0^5 - q_3w_0^3 + q_5w_0)}{(q_1w_0^5 - q_3w_0^3 + q_5w_0)^2 + (q_2w_0^4 - q_4w_0^2 + q_6)^2}\right) \tag{5.18}$$

In order to establish conditions for a Hopf bifurcation to occur at τ_0 , we need to compute the sign of $\frac{d[Re(\lambda)]}{d\tau}$. Differentiating the characteristic equation (5.14) with respect to τ gives

$$\left[6\lambda^5 + 5p_1\lambda^4 + 4p_2\lambda^3 + 3p_3\lambda^2 + 2p_4\lambda + p_5 + e^{-\lambda\tau}(5q_1\lambda^4 + 4q_2\lambda^3 + 3q_3\lambda^2 + 2q_4\lambda + q_5)\right]\frac{d\lambda}{d\tau} -$$
$$e^{-\lambda\tau}\tau(q_1\lambda^5 + q_2\lambda^4 + q_3\lambda^3 + q_4\lambda^2 + q_5\lambda + q_6)\frac{d\lambda}{d\tau} = \lambda(q_1\lambda^5 + q_2\lambda^4 + q_3\lambda^3 + q_4\lambda^2 + q_5\lambda + q_6)e^{-\lambda\tau}$$

$$\frac{d\tau}{d\lambda} = \frac{6\lambda^5 + 5p_1\lambda^4 + 4p_2\lambda^3 + 3p_3\lambda^2 + 2p_4\lambda + p_5 + e^{-\lambda\tau}(5q_1\lambda^4 + 4q_2\lambda^3 + 3q_3\lambda^2 + 2q_4\lambda + q_5)}{\lambda(q_1\lambda^5 + q_2\lambda^4 + q_3\lambda^3 + q_4\lambda^2 + q_5\lambda + q_6)e^{-\lambda\tau}} - \frac{\tau}{\lambda}$$
$$= \frac{(6\lambda^5 + 5p_1\lambda^4 + 4p_2\lambda^3 + 3p_3\lambda^2 + 2p_4\lambda + p_5)e^{\lambda\tau} + 5q_1\lambda^4 + 4q_2\lambda^3 + 3q_3\lambda^2 + 2q_4\lambda + q_5}{\lambda(q_1\lambda^5 + q_2\lambda^4 + q_3\lambda^3 + q_4\lambda^2 + q_5\lambda + q_6)} - \frac{\tau}{\lambda} \tag{5.19}$$

Taking $\lambda = iw_0$, $\tau = \tau_0$ from (5.19) and using the equations in (5.15), we obtain:

$$Re\left(\frac{d\lambda}{d\tau}\right)^{-1}\Bigg|_{\lambda=iw_0} = \frac{6x^5 + 5d_1x^4 + 4d_2x^3 + 3d_3x^2 + 2d_4x + d_5}{(q_2w_0^4 - q_4w_0^2 + q_6)^2 + (q_1w_0^5 - q_3w_0^3 + q_5w_0)^2} \tag{5.20}$$

For a Hopf bifurcation to occur at τ_0 , the transversality condition

$$\left[\frac{d[Re(\lambda)]}{d\tau}\right]\Bigg|_{\tau=\tau_0} = \frac{6x^5 + 5d_1x^4 + 4d_2x^3 + 3d_3x^2 + 2d_4x + d_5}{(q_2w_0^4 - q_4w_0^2 + q_6)^2 + (q_1w_0^5 - q_3w_0^3 + q_5w_0)^2} \neq 0 \tag{5.21}$$

must hold Tipsri & Chinviriyasit (2015). If $d_5 > 0$, then (5.21) holds. In this case, E_1 is conditionally stable for $0 \leq \tau < \tau_0$ and a family of periodic solutions bifurcates from E_1 as τ passes through the critical-delay value τ_0. That is, E_1 becomes unstable when $\tau > \tau_0$. Which means, system (5.1) undergoes a Hopf bifurcation near E_1 at $\tau = \tau_0$. □

CHAPTER 6

NUMERICAL SIMULATIONS

6.1 Numerical Simulation of the System

In this section, we present numerically the behaviour of the solutions of the system 4.1 and 5.1 for different values of parameters given in the model and explain the impact of parameters and delay period on the spread of coronavirus outbreak. We conducted numerical simulation in order to investigate the effects of the parameters and incubation period on the transmission dynamics of COVID-19. To conduct the study, a set of meaningful values are assigned to the model parameters.

6.2 Parameter Estimations

In this section, we fit the proposed model using real data of COVID-19 infection cases in Ethiopia and we estimate the unknown model parameters. The simulation process are performed using $MATLAB\ R2017b$ software. Table 6.1 depicts the daily real data of total confirmed cases of COVID-19 infection in Ethiopia from 8 July 2022 to 6 August 2022 extracted from Ethiopian Minister of Health situation reports. To solve the dynamic parameter estimation problem, we formulate system 4.1 in the following form

$$y' = f(t, y, \theta), y(t_0) = y_0 \tag{6.1}$$

where y is the vector of dependent variables and θ is the vector of unknown parameters. The error is sum of squares error and is represented by

$$\theta = \sum_{i=1}(y_i - \bar{y}_i)^2 \tag{6.2}$$

The expression $\bar{y}_i(t)$ represents the actual total confirmed cases of COVID-19 and $y_i(t)$ are

Table 6.1: Cumulative confirmed cases of COVID-19 infection from 8 July 2021 to 6 August 2022

No	**Month**	**Total confirmed cases**	**No**	**Month**	**Total confirmed cases**	**No**	**Month**	**Total confirmed cases**
1	8 July	490182	11	18 July	491172	21	28 July	492046
2	9 July	490296	12	19 July	491285	22	29 July	492125
3	10 July	490370	13	20 July	491409	23	30 July	492194
4	11 July	490486	14	21 July	491508	24	31 July	492237
5	12 July	490557	15	22 July	491642	25	1 August	492278
6	13 July	490695	16	23 July	491729	26	2 August	492316
7	14 July	490816	17	24 July	491759	27	3 August	492375
8	15 July	490925	18	25 July	491834	28	4 August	492412
9	16 July	491031	19	26 July	491917	29	5 August	492461
10	17 July	491086	20	27 July	491979	30	6 August	492476

the corresponding model solutions at time t_i . The aim is minimizing objective function

$$minE(\theta) \quad subject \quad to \quad Equation \quad 6.1 \tag{6.3}$$

to obtain our parameter estimates. In the process of least-squares fitting, we are looking for a value $\bar{\theta}$ of model parameter θ such that the squared sum of errors is the minimum. Clearly, such a problem is nonlinear least squares problem, since the dependence of a solution $y(t, \theta)$ on the parameter θ is through a highly nonlinear system of differential equations. The parameter estimation algorithm is written below:

The model parameters of the model system (4.1) are estimated using least-square fitting

Algorithm 1 Parameter estimation

1: Guess initial parameter values θ_0 . Set $\theta = \theta_0$.

2: Using MATLAB ode23s solver, solve equation 6.1 using θ to solve the solution of the system.

3: Evaluate error using equation 6.2.

4: Check convergence criteria. If not converged go to 2.

5: On convergence, set $\theta = \bar{\theta}$ to current parameter values.

methods which provides a better fit for the model solution to the real data as shown in figure 6.1 and the corresponding parameters value are depicted in Table 6.2 below for the numerical simulation.

In the next section, we study the dynamics of COVID-19 through numerical simulations by

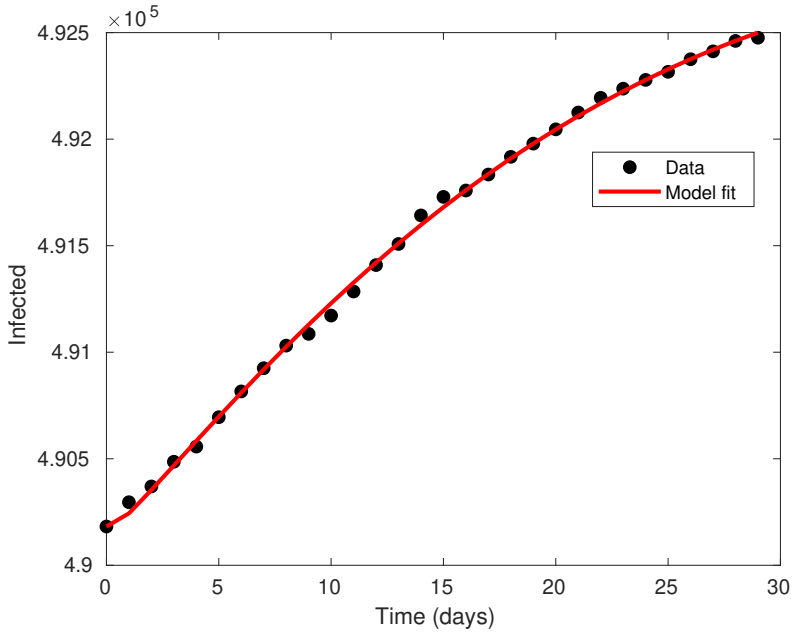

Figure 6.1: SVEAIR model fit with real data on the number of COVID-19 cases in Ethiopia

using the fitted values of parameters in the proposed model with appropriate initial conditions with the help of least square method.

6.3 Simulation Results and Discussion

In this section, we present numerical simulations to support the theoretic analysis of both the ODE(4.1) and DDE (5.1) models given in the previous sections using the parameters values listed in Table 6.2.

6.3.1 Simulation Results and Discussion for Deterministic Mathematical Model

In this section, we illustrate numerically the solution of the problem proposed in system 4.1 and explain the impact of parameters on reproduction number (R_0) on the spread of corona virus diseases.

To perform the numerical simulation, we assumed the initial population of $(E(0), A(0)) = (2435303, 618450)$ and the remaining $V(0) = 42797649,\ \ I(0) = 490182,\ \ R(0) = 466389$ from the collected real data. Also the initial susceptible population is obtained from $S(0) = N(0) - (V(0) + E(0) + A(0) + I(0) + R(0)) = 74201298$ and the total population of Ethiopia up to 16 August 2022 is $N(0) = 121279271$ (United Nation data on country meter). The natural death rate is computed as $\mu = 1/(56.24 \times 12 \times 30)$ per day, where 56.24 years (United Nation data on country meter) is the average life expectancy in Ethiopia . The recruitment rate, is then calculated as $\Lambda = \mu \times N(0) = 5994$ per day.

The model parameters of the model system 4.1 are estimated using least-square fitting methods which provides a better fit for the model solution to the real data as shown in figure and the corresponding parameters value are depicted in Table below for the numerical simulation.

The estimation of basic reproduction number for the model is given by

$$R_0 = \frac{\beta\kappa(\phi+\mu)(q(1-\rho)(\mu+\alpha+\delta)+\rho(\gamma+\mu))}{(\kappa+\mu)(\gamma+\mu)(\mu+\alpha+\delta)(\phi+\psi+\mu)} = 1.5087 > 1$$

Table 6.2: The values of parameters used in the simulations

Parameter	Description	value	Reference
Λ	Recruitment rate	5994(per day)	Estimated
β	Effective contact rate of infection	0.92	fitted
κ	Per capita rate of becoming infectious	0.1249	fitted
q	Transmission rate for asymptomatic individuals	0.4722	fitted
ρ	Probability of exposed individuals joining infectious class	0.9692	fitted
α	Progression from compartment $I(t)$ to $R(t)$ due to effective treatment	0.5001(per day)	fitted
δ	Death rate due to disease in the symptomatic compartment	0.00021(per day)	fitted
ϕ	The rate vaccine wanes	0.4231(per day)	fitted
ψ	The transmission rate of susceptible into vaccinated class	0.0891(per day)	fitted
γ	Rate at which asymptomatic individuals recovered	0.2970(per day)	fitted
μ	Natural death rate	0.0000494266(per day)	fitted
θ	Rate at which recovered individuals reverts to susceptible class	0.00124 (per day)	fitted

Since $R_0 > 1$, the prevalence of COVID-19 will result in an epidemic.

Figure 6.2a indicates that the endemic equilibrium point is locally asymptotically stable if $R_0 > 1$. In another way, by changing the values of ϕ and ψ only, then $R_0 < 1$. This suggests that vaccines have a significant impact on COVID-19 disease reduction. As a result, vaccination is one of the disease dynamics' control mechanisms. Let us suppose the values of ϕ and ψ are 0.231 and 0.3891, respectively. Then, as figure 6.2b indicates, the disease free equilibrium point is locally asymptotically stable for $R_0 < 1$.

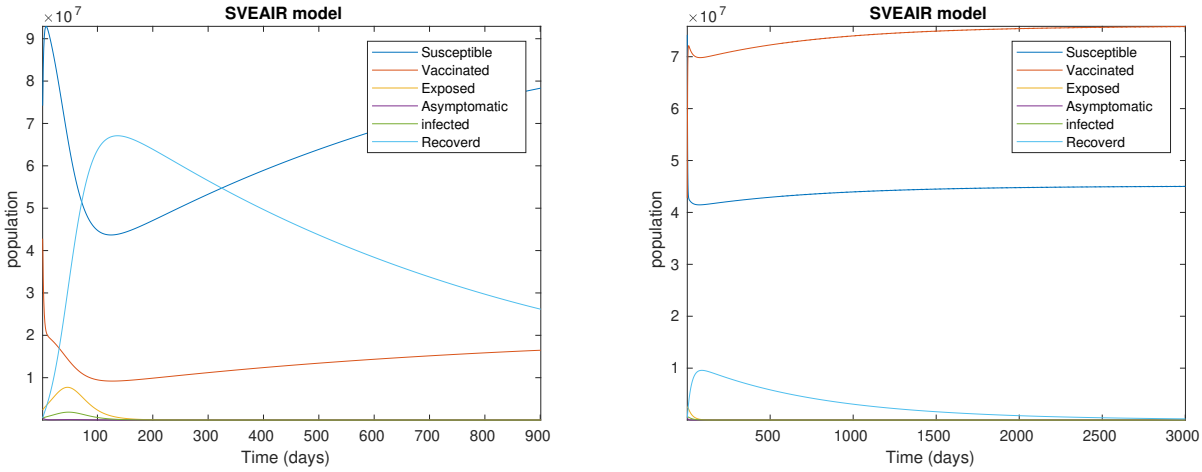

(a) (b)

Figure 6.2: a) SVEAIR model with $R_0 > 1$ b) SVEAIR model with $R_0 = 0.6803$

6.3.2 Simulation Results and Discussion for DDEs Model

To support the analytical findings presented in model 5.1, we run numerical simulations in this section. For DDEs, we employ the same initial conditions and parameters stated in ODEs. The disease free equilibrium is locally asymptotically stable for $R_0 < 1$ for all $\tau > 0$ with the following parameters and the same initial conditions with non delay part: $\beta = 0.92$, $q = 0.4722$, $\Lambda = 5994$, $\theta = 0.00124$, $\psi = 0.3891$, $\phi = 0.231$, $\mu = 0.0000494266$, $\kappa = 0.1249$, $\rho = 0.9692$, $\gamma = 0.2970$, $\alpha = 0.5001$, $\delta = 0.00021$, $N = 121279271$. In other situations, the endemic equilibrium becomes unstable and changes into the equilibrium point for a disease free. This shows that the incubation period has a negative effect on disease pandemic. The disease's ability to spread more and more slowly as time delay increases. The figure 6.3a indicate that the disease free equilibrium point and figure 6.3b show as the endemic equilibrium point analyzation with $\beta = 0.92$, $q = 0.4722$, $\Lambda = 5994$, $\theta = 0.00124$, $\psi = 0.0891$, $\phi = 0.4231$, $\mu = 0.0000494266$, $\kappa = 0.1249$, $\rho = 0.9692$, $\gamma = 0.2970$, $\alpha = 0.5001$, $\delta = 0.00021$, $N = 121279271$.

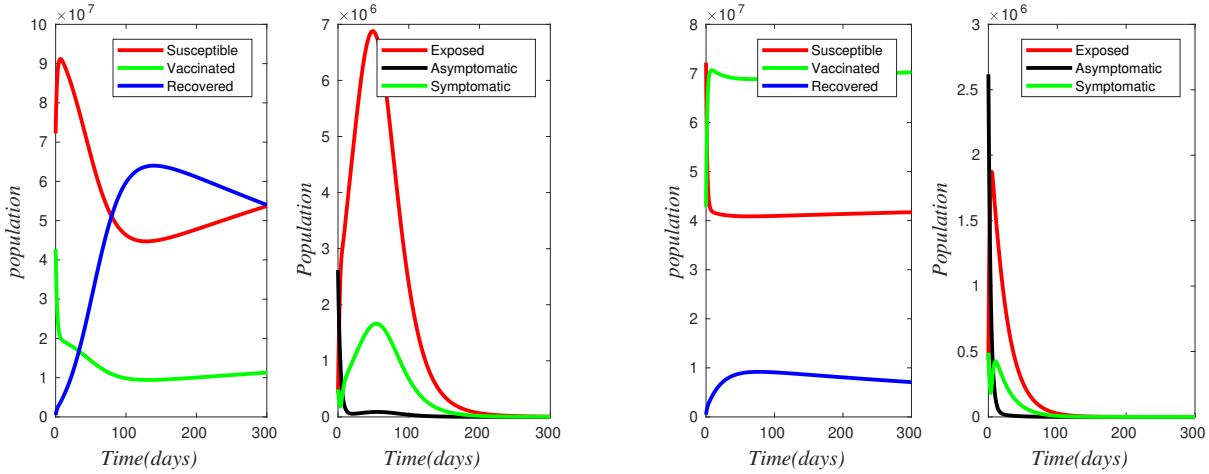

(a) (b)

Figure 6.3: a) Delay SVEAIR model with $R_0 > 1$ b) Delay SVEAIR model with $R_0 = 0.6803$

Existence of Hopf bifurcation

In this section, we prove the existence of hopf bifurcation by changing the value of κ in Table 4.2. As κ increases the value of R_0 also increase figure (4.2). By taking the same initial condition (S, V, E, A, I, R)=(74221298, 42797649, 3155303, 148450, 490182, 466389), $\beta = 0.88$, $q = 0.4722$, $\Lambda = 5994$, $\theta = 0.00124$, $\phi = 0.245$, $\psi = 0.431$, $\mu = 0.00004943$, $\kappa = 0.5249$, $\rho = 0.9692$, $\gamma = 0.1970$, $\alpha = 0.3001$, $\delta = 0.00021$, $N = 121279271$. This parameters and initial conditions implies that $R_0 > 1$. Let us see by cases for different values of τ by considering $t \in [0, 300]$. If the time tends to infinity the DDEs model becomes ODEs model.

a) The Case of $\tau > \tau_0$

The delay will increase as the incubation period increases. Once the delay exceeds the threshold value, the pandemic dynamic system is at risk of instability. The stability of the equilibrium point is simulated when $\tau = 4.5 > \tau_0$ in figure 6.6. The values of the parameters are the same. The equilibrium is unstable within 300 days. To show the stability of the equilibrium point when $\tau = 4.5$ more clearly, the system is unstable. This implies that the endemic equilibrium has lost its stability.

b) The Case of $\tau < \tau_0$

The delay will get shorter as the incubation time gets shorter. When $\tau = 3.9 < \tau_0$, the stability of equilibrium point is simulated in figure 6.4. The parameters have the same values. Despite the fact that $R_0 > 1$ suggests that the endemic equilibrium is asymptotically stable,

the disease free equilibrium point is stable. As a result, the graph gets closer to the free disease equilibrium point. As a result, we draw the conclusion that the hopf bifurcation occurs at $\tau_0 = 4$ figure 6.5. While we obtain a stable equilibrium point for $\tau = 3.9 < 4$, we obtain an unstable equilibrium point for $\tau = 4.5 > 4$.

In general, the incubation period has the highest impact on COVID-19 propagation. As the time increases, the DDEs system becomes ODEs. With no time delay (incubation period), the system does not indicate the reality behind COVID-19. That means, for studying transmission of COVID-19, exposed individuals do not transmit the disease immediately. There is an incubation period which is (3-5)days. In our simulation result, the incubation period considered is within this interval. Further more let us check by extending time interval to discuss the stability and behavior of time delay model. With initial conditions $(S, V, E, A, I, R) = (94201298, 42797649, 505303, 2618450, 490182, 466389)$ and parameters $\beta = 0.92; q = 0.4722, \Lambda = 5994, \theta = 0.00124, \phi = 0.4231, \psi = 0.0891, \mu = 0.0000494266, \kappa = 0.1249, \rho = 0.9692, \gamma = 0.2970, \alpha = 0.5001, \delta = 0.00021, N = 121279271$. If a time interval is increased the endemic equilibrium point is locally asymptotically stable as $\tau = 3$ figure (6.7). When we increasing incubation period to ($\tau = 15$) the endemic equilibrium loss it is stability figure(6.8). As this incubation period we have hopf bifurcation. Also as incubation period becomes 18 it is also not stable figure(6.9) and does not exist for above 18 as we see figure (6.10) as $\tau = 19$.

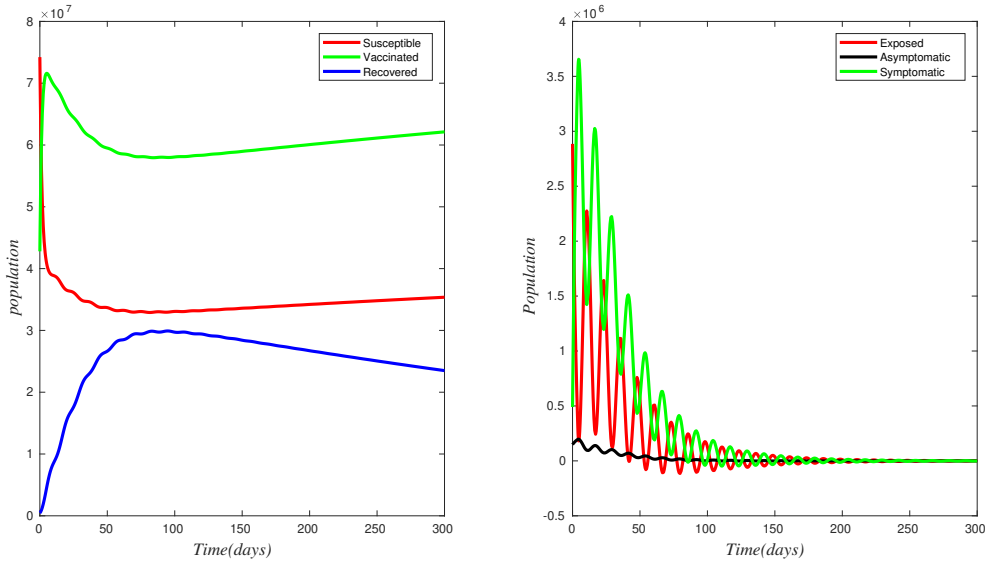

Figure 6.4: The stable equlibrium point at $\tau = 3.9 < 4$.

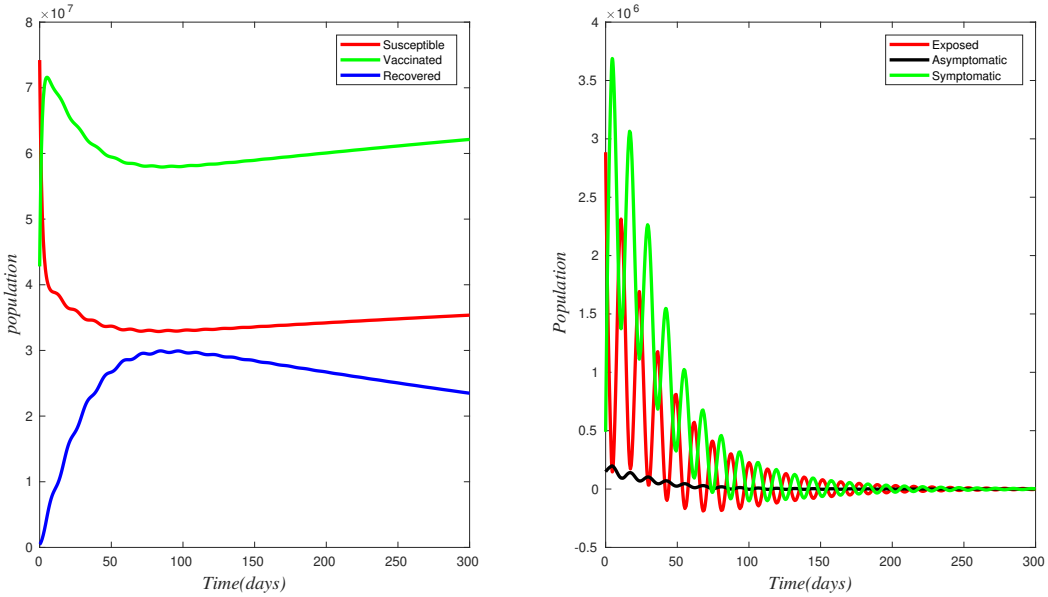

Figure 6.5: The existence of hopf-bifurcation at $\tau = 4$.

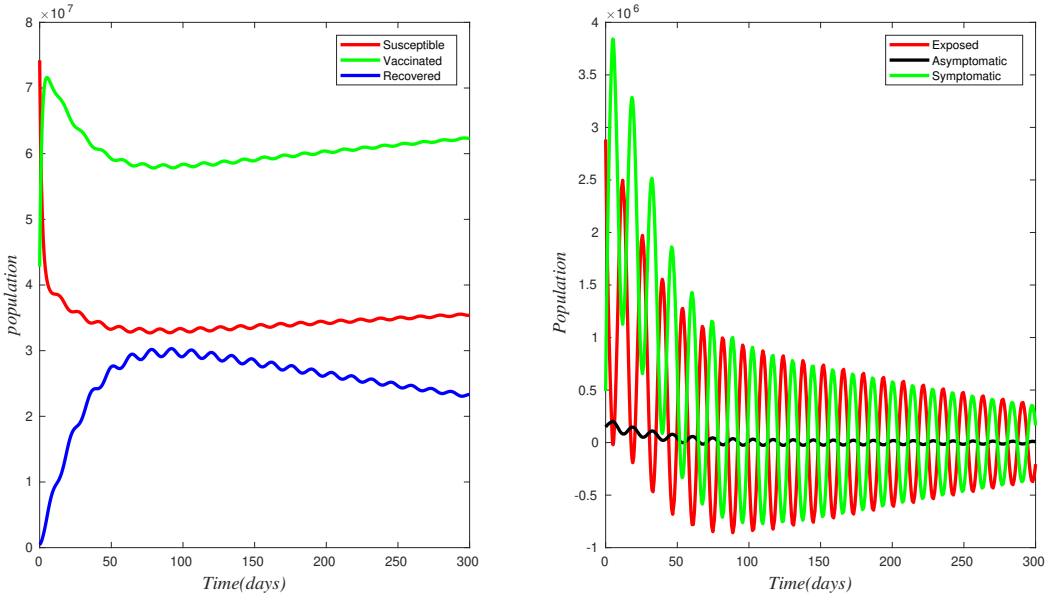

Figure 6.6: The existence of unstable equilibrium point at $\tau = 4.5 > 4$.

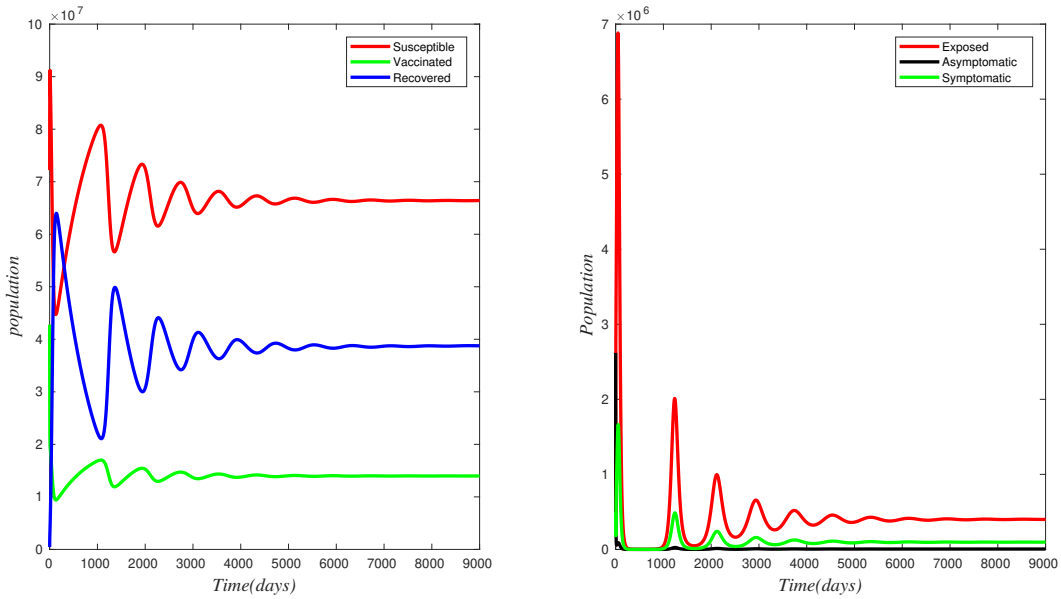

Figure 6.7: Endemic equlibrium point exist and stable at time interval $\tau = 3$

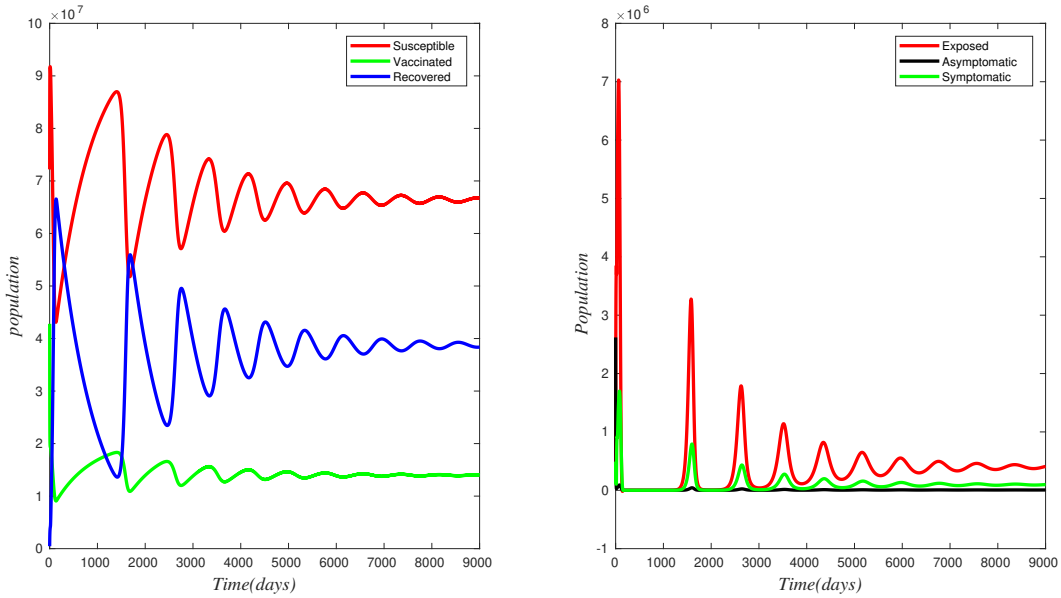

Figure 6.8: Endemic equilibrium loss it is stablity at incubation period is 15.

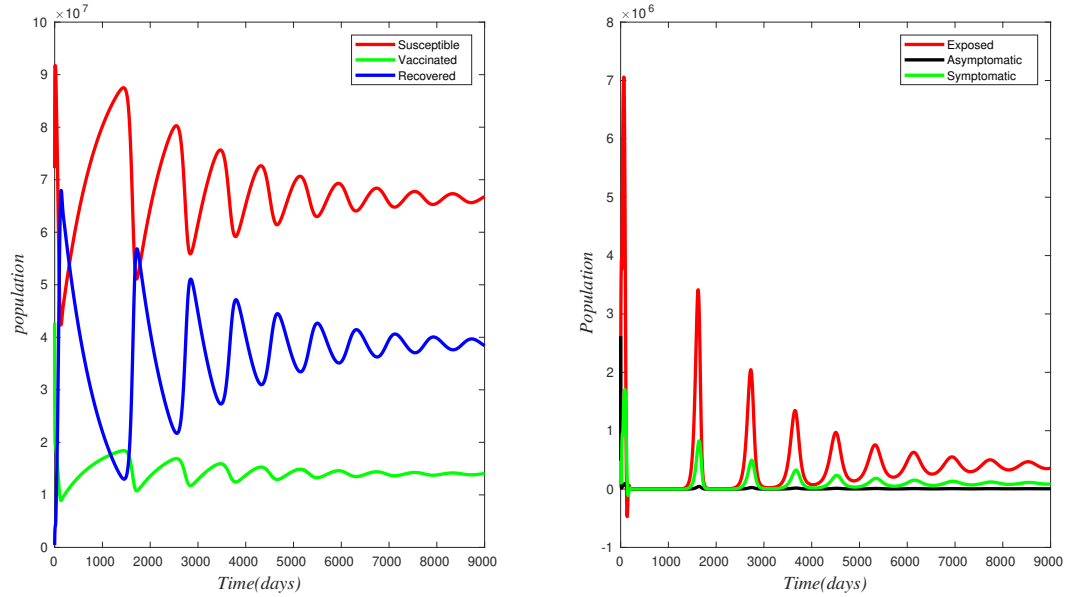

Figure 6.9: The endemic equlibrium point at $\tau = 18$

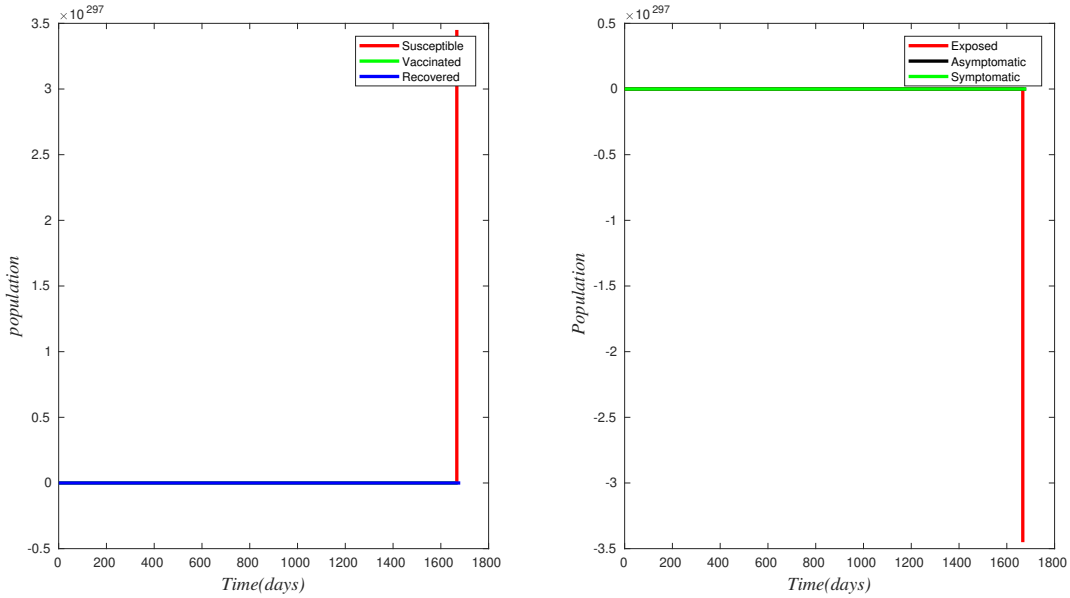

Figure 6.10: The stability of endemic equlibrium point at $\tau = 19$

CHAPTER 7

RESULT AND DISCUSSION

7.1 Result and Discussion

In this thesis work, we have considered COVID-19 disease. We have developed a six compartmental epidemic model, namely susceptible, vaccinated, exposed, asymptomatic, symptomatic, and recovered populations. The well-posedness of the model was established in both the mathematical and epidemiological senses by showing that all solutions of the model are positive and bounded with initial conditions.

We have discussed the invariant region. Using the next generation matrix method, we have found

$$R_0 = \frac{\beta q \kappa (1-\rho)(\alpha+\mu+\delta)(\phi+\mu) + \beta\kappa\rho(\gamma+\mu)(\phi+\mu)}{(\gamma+\mu)(\kappa+\mu)(\mu+\alpha+\delta)(\phi+\psi+\mu)}$$

as basic reproduction number of the system, which helps us to determine the dynamical behavior of the system.

We have established two distinct equilibriums for the model with both local and global stability on the disease-free and endemic equilibrium points. The system 4.1 is locally asymptotically stable at the disease free equilibrium point E_0 when $R_0 < 1$. When $R_0 > 1$, the endemic equilibrium E_1 exists and the system becomes unstable at E_0 and locally asymptotically stable at E_1.

This thesis' main goal is to look into COVID-19's delayed dynamical model. We focused on the incubation period, which is the amount of time between exposure and infection. The basic reproduction number (R_0) is found to be greatly affected by time delay, which suggests that the endemic equilibrium loses its stability and shifts to a disease-free equilibrium point.

Thus, by changing the parameters and initial values, the model exhibits hopf bifurcation at the endemic equilibrium point. The numerical simulation of the model systems 4.1 and 5.1 has been performed, and the simulation process is carried out using the software MATLAB R2017b. We also found the value of the parameters using least-square fitting methods with the software MATLAB R2017b.

CHAPTER 8

CONCLUSSION AND RECOMMENDATION

8.1 Conclussion

In this thesis work, first we develop a mathematical model which describes the transmission dynamics of COVID-19 using a system of nonlinear ordinary differential equations. The well-possedness of the model was established both in the mathematical and epidemiological senses by showing that all solutions of the model are positive and bounded with initial conditions in a certain sense.

We performed a qualitative analysis of the model. Both local and global stability analyses of the equilibrium points of the model equations have been done using Jacobian matrix and Lyapunov functions, respectively. Sensitivity analysis of the model has been studied and determined a parameter which plays a greater role in the transmission dynamics of COVID-19 disease.

The proposed mathematical model is extended to the delayed dynamical model. Here we have used one delay period for the incubation period. Then, the invariant region, the positevity, boundedness of the model, the reproduction number, and the equilibrium points of our model were derived and investigated. The qualitative analysis indicated that the covid free equilibrium point is locally and globally stable for $R_0 < 1$, while the endemic equilibrium point is locally stable or may have hopf bufarication at $R_0 > 1$, depending on initial conditions, parameters, and incubation period. Also, the incubation period has a negative impact on the disease pandemic.

Finally, different simulation cases were comparatively performed. The numerical simulation results demonstrate good agreement with our analytical results. The simulation results also clearly shown that the COVID-19 can be minimized by reducing the parameters that have positive impact on disease pandemic and increasing the values of parameters which have the negative impact on COVID-19 pandemic.

8.2 Recommendation

Controlling the spread of an epidemic disease is currently a difficult and crucial research topic. Finding the dynamics of disease transmission and predicting its future are crucial for disease control. Therefore, as we can see from the above, administering the vaccine to susceptible people is easier and more efficient. The findings of this study advise every one to get the COVID-19 vaccine because it is still difficult to eradicate the disease, particularly in developing nations. Additionally, we advise that the government treat those who are already ill and contagious and administer the right vaccination to those who are susceptible. Finally, I urge academics, particularly those in Ethiopia, to learn more about delays in order to look into the more accurate prediction of infectious diseases.

8.3 Future Work

In future work, we plan to extend the study of this model by incorporating optimal control into the system. We also transform deterministic mathematical models into stochastic mathematical models to make them more realistic.

References

Alfarouk, K. O., AlHoufie, S. T., Ahmed, S., Shabana, M., Ahmed, A., Alqahtani, S. S., ... others (2021). Pathogenesis and management of covid-19. *Journal of Xenobiotics*, *11*(2), 77–93.

Almeida, J., Berry, D., Cunningham, C., Hamre, D., Hofstad, M., Mallucci, L., ... Tyrrell, D. (1968). *Coronaviruses* (Vol. 220) (No. 5168). NATURE PUBLISHING GROUP MACMILLAN BUILDING, 4 CRINAN ST, LONDON N1 9XW, ENGLAND.

Almocera, A. E. S., Quiroz, G., & Hernandez-Vargas, E. A. (2021). Stability analysis in covid-19 within-host model with immune response. *Communications in Nonlinear Science and Numerical Simulation*, *95*, 105584.

Anderson, R. M., & May, R. M. (1992). *Infectious diseases of humans: dynamics and control*. Oxford university press.

Annas, S., Pratama, M. I., Rifandi, M., Sanusi, W., & Side, S. (2020). Stability analysis and numerical simulation of seir model for pandemic covid-19 spread in indonesia. *Chaos, Solitons & Fractals*, *139*, 110072.

Araz, S. İ. (2021). Analysis of a covid-19 model: optimal control, stability and simulations. *Alexandria Engineering Journal*, *60*(1), 647–658.

Bhadauria, A. S., Pathak, R., & Chaudhary, M. (2021). A siq mathematical model on covid-19 investigating the lockdown effect. *Infectious Disease Modelling*, *6*, 244–257.

Çakan, S. (2020). Dynamic analysis of a mathematical model with health care capacity for covid-19 pandemic. *Chaos, Solitons & Fractals*, *139*, 110033.

Carli, R., Cavone, G., Epicoco, N., Scarabaggio, P., & Dotoli, M. (2020). Model predictive control to mitigate the covid-19 outbreak in a multi-region scenario. *Annual Reviews in Control*.

Carr, J. (2012). *Applications of centre manifold theory* (Vol. 35). Springer Science & Business Media.

Castillo-Chavez, C., & Song, B. (2004). Dynamical models of tuberculosis and their applications. *Mathematical Biosciences & Engineering*, *1*(2), 361.

Centers, D. C., Prevention, et al. (2020). *Symptoms of coronavirus.*

Chernet, T. D., Yesuf, O. M., & Gemechis, F. D. (2020). Optimal control and sensitivity analysis for transmission dynamics of coronavirus. *Results in Physics*, *19*, 103642.

Chitnis, N., Hyman, J. M., & Cushing, J. M. (2008). Determining important parameters in the spread of malaria through the sensitivity analysis of a mathematical model. *Bulletin of mathematical biology*, *70*(5), 1272–1296.

Davis, B. N., Hilyard, A. C., Lagna, G., & Hata, A. (2008). Smad proteins control drosha-mediated microrna maturation. *Nature*, *454*(7200), 56–61.

Diekmann, O., Heesterbeek, J. A. P., & Metz, J. A. (1990). On the definition and the computation of the basic reproduction ratio r 0 in models for infectious diseases in heterogeneous populations. *Journal of mathematical biology*, *28*(4), 365–382.

Ebraheem, H. K., Alkhateeb, N., Badran, H., & Sultan, E. (2021). Delayed dynamics of sir model for covid-19. *Open Journal of Modelling and Simulation*, *9*(2), 146–158.

Forni, D., Cagliani, R., Clerici, M., & Sironi, M. (2017). Molecular evolution of human coronavirus genomes. *Trends in microbiology*, *25*(1), 35–48.

Ghostine, R., Gharamti, M., Hassrouny, S., & Hoteit, I. (2021). An extended seir model with vaccination for forecasting the covid-19 pandemic in saudi arabia using an ensemble kalman filter. *Mathematics*, *9*(6), 636.

Giordano, G., Blanchini, F., Bruno, R., Colaneri, P., Di Filippo, A., Di Matteo, A., & Colaneri, M. (2020). Modelling the covid-19 epidemic and implementation of population-wide interventions in italy. *Nature medicine*, *26*(6), 855–860.

Gurmu, E. D., Batu, G. B., & Wameko, M. S. (2020). Mathematical model of novel covid-19 and its transmission dynamics. *International Journal of Mathematical Modelling & Computations*, *10*(2 (SPRING)), 141–159.

Hale, J. K., & Lunel, S. M. V. (2013). *Introduction to functional differential equations* (Vol. 99). Springer Science & Business Media.

Hethcote, H. W. (2000). The mathematics of infectious diseases. *SIAM review*, *42*(4), 599–653.

Huang, W., Cooke, K. L., & Castillo-Chavez, C. (1992). Stability and bifurcation for a multiple-group model for the dynamics of hiv/aids transmission. *SIAM Journal on Applied Mathematics*, *52*(3), 835–854.

Ivorra, B., Ferrández, M. R., Vela-Pérez, M., & Ramos, A. M. (2020). Mathematical modeling of the spread of the coronavirus disease 2019 (covid-19) taking into account the undetected infections. the case of china. *Communications in nonlinear science and numerical simulation*, *88*, 105303.

Kermack, W. O., & McKendrick, A. G. (1927). A contribution to the mathematical theory of epidemics. *Proceedings of the royal society of london. Series A, Containing papers of a mathematical and physical character*, *115*(772), 700–721.

Lalchhandama, K. (2020). The chronicles of coronaviruses: the bronchitis, the hepatitis and the common cold. *Scienc e Vision*, *1*, 43–53.

La Salle, J. P. (1976). The stability of dynamical systems. *SIAM*.

Layek, G. (2015). *An introduction to dynamical systems and chaos* (Vol. 449). Springer.

Lenhart, S., & Workman, J. T. (2007). *Optimal control applied to biological models*. CRC press.

Li, M. Y. (2018). *An introduction to mathematical modeling of infectious diseases* (Vol. 2). Springer.

Li, Y., & Zhang, Q. (2020). The balanced implicit method of preserving positivity for the stochastic siqs epidemic model. *Physica A: Statistical Mechanics and its Applications*, *538*, 122972.

Maleewong, M. (2020). Time delay epidemic model for covid-19. *medRxiv*.

Menendez, J. (2020). Elementary time-delay dynamics of covid-19 disease. *medRxiv*.

Merkin, D. R. (1997). Stability of linear autonomous systems. In *Introduction to the theory of stability* (pp. 133–158). Springer.

Monto, A. S. (1989). Coronaviruses. In *Viral infections of humans* (pp. 153–167). Springer.

Nisar, K. S., Ahmad, S., Ullah, A., Shah, K., Alrabaiah, H., & Arfan, M. (2021). Mathematical analysis of sird model of covid-19 with caputo fractional derivative based on real data. *Results in Physics*, *21*, 103772.

Odagaki, T. (2021). Exact properties of siqr model for covid-19. *Physica A: Statistical Mechanics and its Applications*, *564*, 125564.

Palmenberg, A. C., Spiro, D., Kuzmickas, R., Wang, S., Djikeng, A., Rathe, J. A., ... Liggett, S. B. (2009). Sequencing and analyses of all known human rhinovirus genomes reveal structure and evolution. *Science*, *324*(5923), 55–59.

Paré, P. E., Beck, C. L., & Başar, T. (2020). Modeling, estimation, and analysis of epidemics over networks: An overview. *Annual Reviews in Control*.

Perko, L. (2013). *Differential equations and dynamical systems* (Vol. 7). Springer Science & Business Media.

Ramos, A., Ferrández, M., Vela-Pérez, M., Kubik, A., & Ivorra, B. (2021). A simple but complex enough θ-sir type model to be used with covid-19 real data. application to the case of italy. *Physica D: Nonlinear Phenomena*, *421*, 132839.

Saldaña, F., Flores-Arguedas, H., Camacho-Gutiérrez, J. A., & Barradas, I. (2020). Modeling the transmission dynamics and the impact of the control interventions for the covid-19 epidemic outbreak. *Mathematical Biosciences and Engineering*, *17*(4), 4165–4183.

Salkeld, D. J., Salathé, M., Stapp, P., & Jones, J. H. (2010). Plague outbreaks in prairie dog populations explained by percolation thresholds of alternate host abundance. *Proceedings of the National Academy of Sciences*, *107*(32), 14247–14250.

Sanchez, M. A., & Blower, S. M. (1997). Uncertainty and sensitivity analysis of the basic reproductive rate: tuberculosis as an example. *American journal of epidemiology*, *145*(12), 1127–1137.

Tipsri, S., & Chinviriyasit, W. (2015). The effect of time delay on the dynamics of an seir model with nonlinear incidence. *Chaos, solitons & fractals*, *75*, 153–172.

Van den Driessche, P., & Watmough, J. (2002). Reproduction numbers and sub-threshold endemic equilibria for compartmental models of disease transmission. *Mathematical biosciences*, *180*(1-2), 29–48.

Wertheim, J. O., Chu, D. K., Peiris, J. S., Kosakovsky Pond, S. L., & Poon, L. L. (2013). A case for the ancient origin of coronaviruses. *Journal of Virology*, *87*(12), 7039–7045.

WHO. (2020a). *https://www.world health organization.info/world-population/ethiopia-population/.*

WHO. (2020b). Pneumonia of unknown cause—china. 2020. *Available at: who. int/csr/don/05-january-2020-pneumonia-of-unkown-cause-china/en/. Accessed April*, *1*.

Worldbank. (2020). *https://www.worldbank.org/en/country/ethiopia/overview.*

Zhang, Z. (2020). A novel covid-19 mathematical model with fractional derivatives: Singular and nonsingular kernels. *Chaos, Solitons & Fractals*, *139*, 110060.

Zhu, C.-C., & Zhu, J. (2021). Dynamic analysis of a delayed covid-19 epidemic with home quarantine in temporal-spatial heterogeneous via global exponential attractor method. *Chaos, Solitons & Fractals*, *143*, 110546.

APPENDICES

sample Matlab code

```
clear all
set(0, 'defaulttextinterpreter','Latex');
%This function solves the delay covid-19 model using dde23
   and then
%produces graphs of the solutions in different window
%Author Boka M.
%First paper for msc thesis
%Adama Science and Technology University,Department of
   Applied Mathematics
%Optimization group, 2020/21 A.Y
function sol = covidwithdelay3new
%%
%y(1) is S(Susceptible)
%y(2) is V(Vaccinated)
%y(3) is E(Exposed)
%y(4) is A(Asymptomatic)
%y(5) is I(infected)
%y(6) is R(Recoverd)
global tau1
tau1=3;
sol = dde23(@ddes, tau1, [74201298; 42797649; 2435303;
   618450; 490182; 466389], [0,700]);
clf reset
subplot(121)
plot(sol.x,sol.y(1,:),'r','LineWidth',2.5)
xlabel('Time(days)','FontAngle','italic','FontName','Times
   New Roman','fontsize',14)
ylabel('population','FontAngle','italic','FontName','Times
```

```
   New Roman','fontsize',14)
hold on
plot(sol.x,sol.y(2,:),'g','LineWidth',2.5)
plot(sol.x,sol.y(6,:),'b','LineWidth',2.5)
legend('Susceptible' ,'Vaccinated', 'Recovered')
subplot(122)
plot(sol.x,sol.y(3,:),'r','LineWidth',2.5)
xlabel('Time(days)','FontAngle','italic','FontName','Times
   New Roman','fontsize',14)
ylabel('Population','FontAngle','italic','FontName','Times
   New Roman','fontsize',14)
hold on
plot(sol.x,sol.y(4,:),'k','LineWidth',2.5)
plot(sol.x,sol.y(5,:),'g','LineWidth',2.5)
legend('Exposed', 'Asymptomatic','Symptomatic')
%=========================================
function dydt = ddes(t,y,Z)
% Parameters:
k(11)=0.92; k(12)=0.4722; k(1)=5994; k(2)=0.00124; k(3)
   =0.3891;k(4)=0.231; k(5)=0.0000494266; k(6)=0.1249; k(7)
   =0.9692;
k(8)=0.2970; k(9)=0.5001; k(10)=0.00021; N =121279271;
S = y(1); V = y(2); E = y(3); A = y(4); I = y(5); R = y(6);
Etau1 = Z(3,1);
dSdt = k(1) + k(2)*R + k(3)*V - k(11)*S*(I+k(12)*A)/N - k(4)*
   S - k(5)*S;
dVdt = k(4)*S - (k(3)+k(5))*V;
dEdt = k(11)*S*(I+k(12)*A)/N - k(5)*E - k(6)*Etau1;
dAdt = k(6)*(1-k(7))*Etau1 - (k(5)+k(8))*A;
dIdt = k(6)*k(7)*Etau1 - (k(9)+k(5)+k(10))*I;
dRdt = k(8)*A + k(9)*I - (k(2)+k(5))*R
dydt = [ dSdt; dVdt;dEdt;dAdt; dIdt; dRdt];
```